Identifying critical language planning regions with direct electrical brain stimulation

Gregg A. Castellucci[1,2], Christopher K. Kovach[3], Farhad Tabasi[3], David Christianson[3], Jeremy D.W. Greenlee[3,4], Michael A. Long[1,2*§]

[1]NYU Neuroscience Institute and Department of Otolaryngology, New York University Langone Medical Center, New York, NY 10016 USA
[2]Center for Neural Science, New York University, New York, NY, 10003 USA
[3]Department of Neurosurgery, University of Iowa Hospitals and Clinics, Iowa City, IA, 52242 USA
[4]Iowa Neuroscience Institute, Iowa City, IA, 52242 USA

3 Figures
5 Supplementary Figures
2 Supplementary Tables

* To whom correspondence should be addressed: Michael A. Long (mlong@med.nyu.edu)
§ Lead contact

One-sentence summary: Perturbations of caudal inferior and middle frontal gyri slow reaction times on an interactive speech task, implicating these areas in planning.

Many brain areas exhibit activity correlated with language planning, but how such dynamics contribute to spoken interaction remains unclear. We employed direct electrical stimulation to perturb cortical function in neurosurgical patient-volunteers performing a question-answer task. Stimulating regions underlying speech perception and orofacial movement evoked diverse sensorimotor deficits, while errors consistent with disrupted response planning resulted from perturbations of numerous, largely frontotemporal loci. We then measured reaction time as an indicator of planning effort and found that stimulation could significantly alter answer latency. Sites displaying stimulation-induced slowed behavior were primarily located in caudal middle and inferior frontal gyri, areas that exhibited preparatory-related activity during conversational turn-taking in previous intracranial recordings. Taken together, our findings indicate that these areas constitute a network critical for planning speech.

The brain must precisely coordinate numerous operations related to sensory perception, planning, and motor control to engage in everyday conversation (*1*, *2*). While lesions to a range of brain regions can affect these processes (*3–6*), associating a particular function to a damaged locus is challenging as such injuries are permanent, often spread across several regions, and typically result multiple behavioral symptoms. To rapidly and reversibly perturb specific structures thought to be related to language, clinicians and researchers have instead used direct electrical stimulation (DES) (*7–18*), and analogous approaches have been employed to investigate vocalization in various model organisms (*19–22*). While DES is regularly leveraged to probe speech sensorimotor function (*10*, *13*, *17*, *18*, *23*, *24*), it has been used less extensively to interrogate the cognitive processes responsible for planning spoken language. In particular, past investigations of speech-related planning have implicated a broad set of cortical regions by examining the qualitative effects of DES, such as errors on naming or repetition tasks (*7–9*, *11*, *14*, *16*, *24–26*); consequently, the neural substrates underlying this process and their contribution to naturalistic spoken communication remain underspecified.

We investigated this topic by assessing how DES affects performance on the critical information (CI) task (*27–29*), an interactive paradigm which requires speech perception, articulation, and all processes related to planning a one-word answer (e.g., conceptual structure planning, retrieval of wordforms, phonological encoding) (*30*, *31*) to occur in behaviorally defined epochs (Fig. 1A). To test whether cortical sites (Fig. 1B) were engaged during interactive speech production, 23 neurosurgical participants (table S1) answered a verbally presented battery of 28 to 143 CI questions (65 ± 21, mean ± SD) as quickly as possible. Meanwhile, we perturbed neural function at 58 total stimulation locations (table S2) with 50 Hz bipolar DES (*7*, *10*) on approximately half of the trials (49 ± 3%; range: 42% - 60%) in an interleaved fashion with control, non-stimulated trials (see Methods). Stimulation intensity ranged from 7.5 to 24 V (15 ± 4 V) across sites, and DES was applied for 3.1 ± 1.0 s during stimulated trials – corresponding to 85 ± 18% of total trial duration and 91± 3% of planning period duration. Therefore, DES was delivered throughout nearly the entire duration of each stimulated trial, allowing us observe the effects of perturbing neural function on CI task performance.

We first observed that cortical stimulation could elicit various sensorimotor disturbances – for example, DES of three sites in participant 494L led to distinct deficits in sensory function and articulatory performance (Fig. 1C-F). Specifically, we found that stimulation of a site within

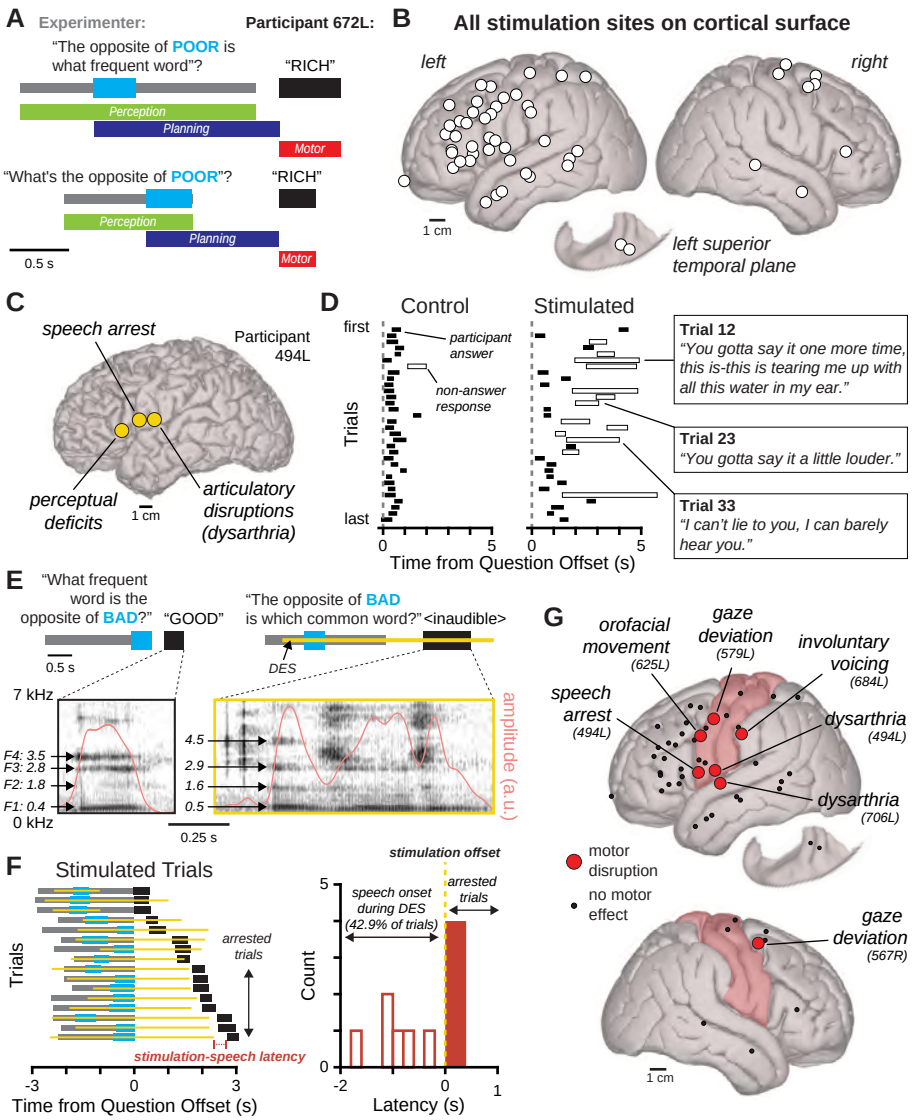

Figure 1. Heterogeneous sensorimotor effects induced by DES. (**A**) Example critical information (CI) questions where the CI is presented early (top) or late (bottom) with behavioral phases indicated. (**B**) Canonical cortical surfaces depicting the position of all stimulation sites across participants; locations of 6 sites in non-surface structures are reported in table S2. (**C**) Left lateral cortical surface of participant 494L with three stimulation sites indicated. (**D**) For the anterior stimulation site in (C), answer timing in control (left) and stimulated trials (middle); example non-answer responses where the participant reported stimulation-induced sensory dysfunction (right). (**E**) Example control trial (left) and trial where stimulation of the posterior site in (C) resulted in articulatory disruption (right); spectrograms of participant response with formant frequencies and envelope amplitude indicated (bottom). (**F**) Schematics of all trials where the middle site in (C) was stimulated (left) with latencies between stimulation and speech onset shown at right. (**G**) Canonical cortical surfaces depicting all sites across participants where stimulation-induced motor effects; data from 6 stimulation sites in non-surface structures did not display motor disruptions (table S2). The location of precentral and postcentral gyri is approximated in light red.

inferior frontal gyrus (Fig. 1C, anterior site) – an area thought to be involved in aspects of spoken language comprehension (*16*, *32–35*) – resulted in disrupted speech perception. Specifically, the participant reported difficulty hearing the question or asked for the question to be repeated on 13 out of 32 stimulated trials but only once on 32 control trials (Fig. 1D). In contrast, stimulation of other sites never resulted in reports of auditory dysfunction or hallucinations and did not exhibit comparable decreases in responsiveness (fig. S1A), including two loci in the vicinity of auditory cortex on the left superior temporal plane (*36–39*) (Fig. 1B). In sum, these results indicate that DES could measurably disrupt sensory-related function during CI task performance.

In the same participant, we found that stimulation of a site in subcentral gyrus (Fig. 1C, posterior site) – a region important for driving speech articulators (*13*, *40*) – resulted in unintelligible speech (i.e., dysarthria; Fig. 1E), which the participant attributed to a perceived stiffness of the orofacial region. Furthermore, stimulation of an additional site in anterior precentral gyrus (Fig. 1C, middle site) induced speech arrest, a well-documented DES-evoked motor deficit (*8*, *9*, *13*, *23*, *24*) proposed to arise from an inability to initiate articulation (*41*). In support of this interpretation, we found that answer onset occurred only 76 - 390 ms (191 ± 124 ms) following stimulation offset on arrested trials (Fig. 1F, fig. S1B,C), which is faster than single word planning times (*42*, *43*) and thus suggests DES prevented the output of a pre-planned answer. Furthermore, we observed additional loci in 5 other participants where stimulation evoked motor effects, including involuntary voicing, gaze deviations, and vocal tract movement (Fig. 1G; table S2). Consistent with previous research (*8–10*, *44–46*), we found that stimulation sites exhibiting such gross motor effects were preferentially located in precentral and postcentral gyri (actual: 86%; mean shuffled: 26 ± 16%) ($p = 0.0007$; permutation test, 100,000 iterations). These results suggest that the observed movement-related deficits resulted from selective perturbation of classic sensorimotor regions as opposed to off-target effects of DES (e.g., via activation of fibers of passage) (*47*, *48*).

We next aimed to identify stimulation-induced behavioral effects related to planning by examining the responses from a participant (640L) possessing a stereo-EEG intracerebral stimulating electrode located in a region of the fusiform gyrus known as the Basal Temporal Language Area (BTLA) (Fig. 2A; table S2). DES of the BTLA can result in anomia (i.e., failure to generate a spoken answer) on various naming tasks, therefore this structure is thought to be critical for semantic access during speech production (*7*, *16*, *49*, *50*). During CI task performance, we found that BTLA stimulation evoked a total of 19 non-sensorimotor speech errors across 32 stimulated trials (Fig. 2B) – including semantic paraphasia (i.e., meaning-related errors; n = 3 trials), anomia (n = 1 trial), and hesitations (i.e., "umm", disfluencies, filler words, see Methods; n = 16 trials with 1 hesitation preceding a semantic error) – while only two errors were observed across 38 control trials (n = 2 hesitations). Importantly, errors contained no gross articulatory disruptions (e.g., Fig. 2B), and BTLA perturbation did not result in neologisms (i.e., phonological errors), suggesting that this region is not involved in planning sound structure or executing articulatory movements. Conversely, these behavioral effects are consistent with stimulation-induced dysfunction in semantic planning, further supporting a role for BTLA in this process while also validating use of the CI task for identifying planning-related loci.

We next analyzed behavioral data from all stimulation sites to determine whether DES outside of BTLA could also induce semantic paraphasia, anomia, and hesitations. We observed several locations that exhibited such errors on stimulated trials (Fig. 2C-E); however, these behaviors were

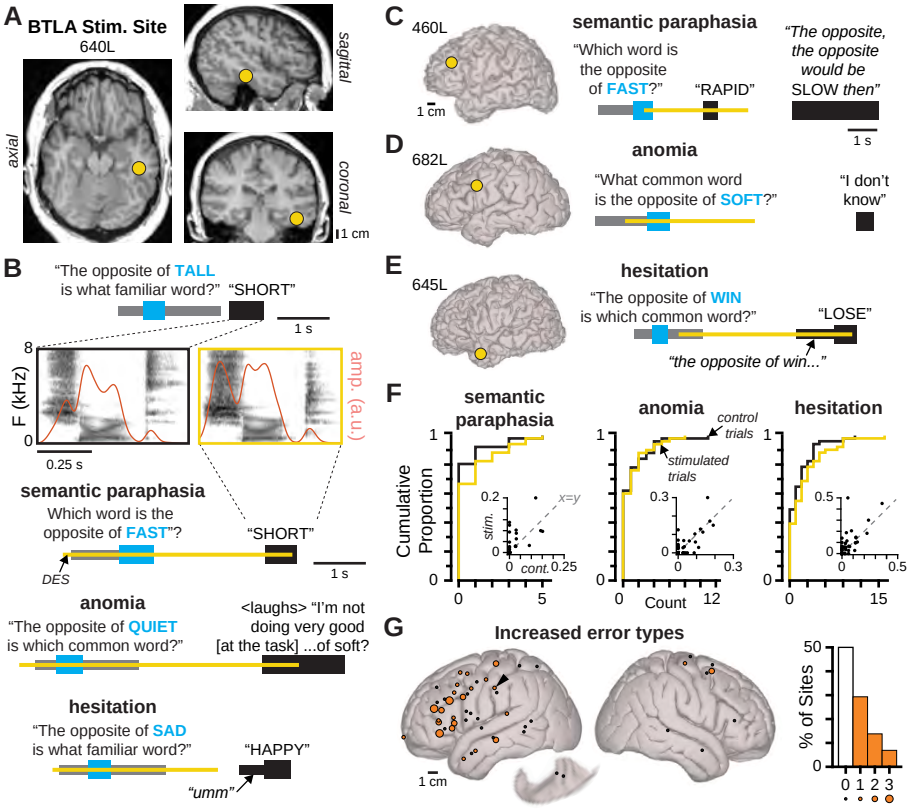

Figure 2. DES can evoke non-sensorimotor speech errors. (**A**) Preoperative magnetic resonance images depicting the stimulation site within the Basal Temporal Language Area (BTLA). (**B**) Example control trial and trials where BTLA stimulation resulted in semantic paraphasia, anomia, and hesitations; spectrograms and envelope amplitude of control and paraphasic responses are also presented. (**C-D**) Example trials from three sites where stimulation induced semantic paraphasia (**C**), anomia (**D**), and hesitations (**E**); site location indicated on participant cortical surfaces at left. (**F**) Cumulative distribution functions of error counts in control and stimulated trials across sites; inset scatterplots depict error rates. (**G**) The percentage of stimulation sites across participants displaying increased rates of one, two, or three error types (right), with corresponding locations depicted on canonical cortical surfaces (left); stimulation of sites in non-surface structures led to increases in either three error types (n = 1; BTLA site), one error type (n = 3), or no error types (n = 2) (table S2). Site displaying stimulation-induced neologisms is indicated with an arrow. Stimulation sites exhibiting motor deficits (see Fig. 1G) were not considered to display increased errors.

both variable and infrequent (Fig. 2F), with only changes in paraphasia and anomia rates being significantly correlated across sites (Pearson's R = 0.45, p = 0.0011) and changes in paraphasia rates displaying a marginal correlation with changes in hesitation rates (Pearson's R = 0.27, p = 0.051). We also assessed whether stimulation evoked phonological errors in our study but observed only a single site displaying an increased rate of neologisms on stimulated trials (table S2; arrow on Fig. 2G). We then examined coregistered data from all participants on a reference brain to determine whether stimulation of specific brain regions elicited speech errors. We found that sites displaying any increase in stimulation-induced errors were broadly distributed across cortex but were largely located within frontal and temporal regions where DES has been reported to elicit paraphasia and anomia (*8*, *9*, *11*, *24*) (Fig. 2G, table S2). Therefore, while we found non-sensorimotor speech errors to be sporadic, these behavioral deficits suggest a broad cortical network potentially related to language planning.

To provide a more reliable metric of planning disruption, we measured the effect of DES on reaction time (RT) – a quantification of planning effort used widely in the fields of psychology, linguistics, and neuroscience (*12*, *51*, *52*). We focused our RT analysis on questions where the CI was presented early in the sentence (e.g., Fig. 1A, top), as these trial variants exhibit the sub-second response latencies characteristic of natural conversation (*1*, *27*, *28*, *53*) and are answered significantly faster than trials where the CI is presented late (e.g., Fig. 1A, bottom; fig. S2A). To first test whether RT could be modulated by DES, we examined the effects of perturbing BTLA on answer timing. Crucially, we found that stimulation of the site within BTLA (Fig. 2A) significantly slowed RT without obviously affecting articulation (Fig. 3A,B; see also Fig. 2B) ($p < 0.0001$, rank-sum test), suggesting that language-related planning processes were selectively disrupted.

We next assessed RT in control and stimulated early trials across all sites where motor disruption did not prevent CI task performance (n = 51; Fig. 3C-F) and observed that stimulation could result in significantly slower RT (n = 9 sites; Fig. 3C), significantly faster RT (n = 3 sites and n = 1 site in late CI trials only; Fig. 3D; table S2), or not affect RT (n = 38 sites; Fig. 3E; fig. S2B). Importantly, these changes in RT were unlikely to have resulted from variability in stimulation intensity, as we found no significant relationship between DES voltage and the probability of observing a stimulation-induced RT alteration (χ^2 vs. constant model: 2.87, p = 0.090; logistic regression). Likewise, the occurrence of RT effects was not related to the participant's clinical condition (χ^2 vs. constant model: 1.12, p = 0.573) or the type of stimulator used (χ^2 vs. constant model: 1.47, p = 0.478) (table S1). In sum, these results demonstrate that RT modulations – both slower and faster – can result from perturbations within a subset of cortical sites likely related to planning.

Because BTLA perturbation (Fig. 2A) resulted in both slower RT (Fig. 3A,B) as well as increased error rates (Fig. 2B), we examined the connection between RT and these behaviors across sites. We found that all locations where stimulation slowed RT exhibited more anomia, paraphasia, and/or hesitations on stimulated trials than control trials, with 6 out of 9 of these sites displaying an increase in at least two error types (fig. S3A; table S2) – significantly more than expected by chance (actual: 67%; mean shuffled: 21 ± 13%) (p = 0.0014; permutation test, 100,000 iterations). Conversely, a consistent trend for increased errors was not observed when stimulation resulted in faster RTs or no effect on RT (fig. S3B,C; table S2). Specifically, faster RT sites did not exhibit a

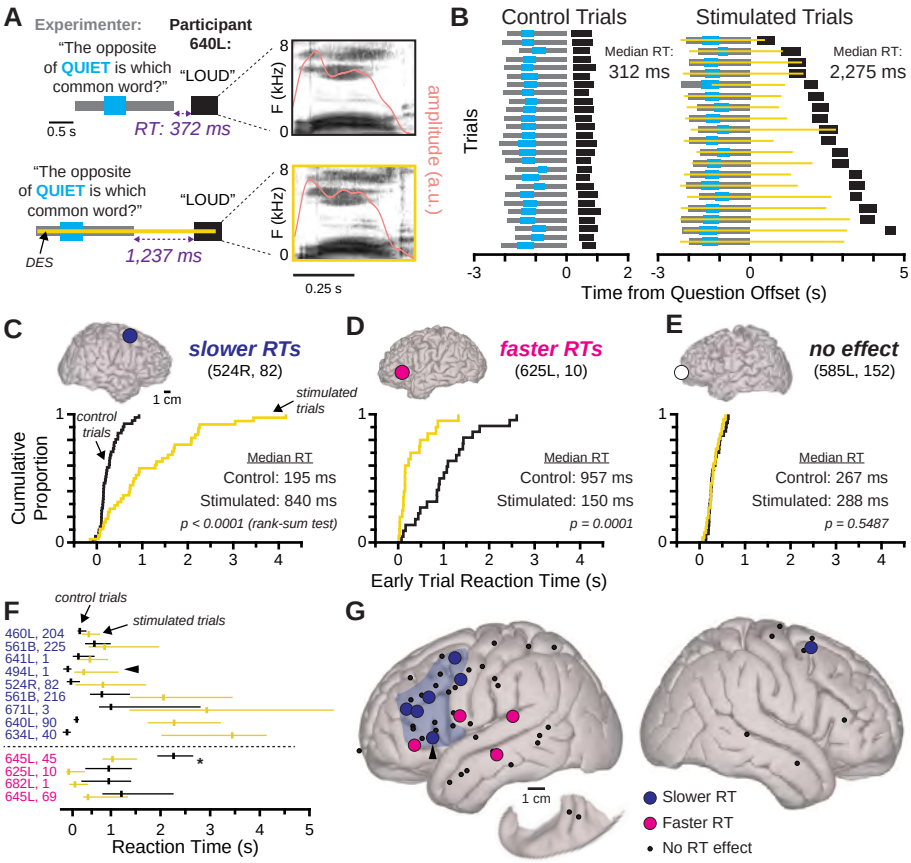

Figure 3. DES-induced reaction time modulations indicate a planning network. (**A**) Example control trial (top left) and trial where the Basal Temporal Language Area (BTLA; see Fig. 2A) was stimulated (bottom left) with reaction times (RT) indicated; spectrograms of participant response with envelope amplitude overlaid (right). (**B**) All control trials and all trials where the site in (A) was stimulated sorted by reaction time. (**C-E**) Empirical cumulative distribution functions of RT for example sites where stimulation induced slower (**C**), faster (**D**), or no statistical difference in RT (**E**); site location indicated on participant cortical surfaces at top. (**F**) Median and interquartile range for all sites where stimulation resulted in significantly slower or faster RT; site where DES induced faster RTs on late CI trials only indicated with an asterisks. (**G**) Canonical cortical surfaces depicting the effect of stimulation on RT in all sites across participants; stimulation of sites in non-surface structures either slowed RT (n = 2; i.e., BTLA and posterior cingulate gyrus) or did not affect RT (n = 4) (table S2). The regions of caudal inferior and middle frontal gyri displaying neural activity related to language planning (*27*) are approximated in light blue. For (F) and (G), the site also displaying stimulation-induced perceptual deficits (Fig. 1C,D) is indicated with an arrow.

comparable increase in two or more error types (50%; p = 0.19; permutation test, 100,000 iterations), and no effect sites displayed fewer such increases than expected (10%, p = 0.012; permutation test, 100,000 iterations). Therefore, disrupted language-related planning via DES is likely signaled by a combination of slower RT and qualitative behavioral deficits including paraphasia, hesitations, and anomia.

Finally, we examined the anatomical distribution of stimulation sites across participants to investigate whether DES-induced RT modulations were spatially organized. We found that sites where stimulation did not affect RT were located broadly across the left and right hemispheres; in contrast, sites exhibiting stimulation-induced increases in RT were primarily restricted to frontal cortical areas (Fig. 3G). Excluding the site in BTLA (Fig. 2A), 7 of these 8 putative planning sites were located in either caudal inferior frontal gyrus (cIFG) (i.e., pars opercularis and pars triangularis) or caudal middle frontal gyrus (cMFG) – significantly more than expected if these sites were randomly distributed (actual: 88%; mean shuffled: 39 ± 16%) (p = 0.004; permutation test, 100,000 iterations) – while a single site was located in left posterior cingulate gyrus (fig. S4; table S2). In our recent electrocorticography investigation of conversational turn-taking, we found that cIFG and cMFG most consistently displayed activity correlated with speech-related planning (*27*), and our stimulation result therefore demonstrates that dynamics in these regions are causally related to this preparatory processing. Furthermore, we previously found that a subregion of IFG overlapping with ventral pars triangularis was active during both speech perception and planning in the CI task; our present results support this mixed function, as the site displaying stimulation-induced perceptual deficits (Fig. 1C,D; arrows in Fig. 3F,G) was located within this area and exhibited both longer reaction times as well as increased error rates in stimulated trials (green in Fig. 3F and fig. S3A). Finally, sites where DES resulted in faster RT (fig. S5) were located outside cIFG and cMFG and not clustered to any specific region of cortex (Fig. 3G), suggesting this phenomenon does not arise from the same mechanism underlying stimulation-induced RT slowing.

In summary, we demonstrate that stimulation of cIFG and cMFG can evoke significantly longer RT and response errors in an interactive task, indicating these structures are critically involved in planning during spoken language production. Left cIFG is a well-known speech-related premotor region classically referred to as "Broca's area", and DES of cIFG has been reported to result in a range of language deficits – including speech arrest, anomia, syntactic errors, semantic paraphasia, neologisms, and disrupted articulation (*8*, *9*, *11*, *24*, *41*, *54*). While differences in patient populations (*8*, *13*, *14*) and study design (*26*) may underlie some variability in stimulation-induced behavioral effects, this region has likewise been linked to multiple linguistic and domain-general cognitive processes (*55–65*). Therefore, cIFG likely represents a heterogenous (*61*, *65*), potentially multimodal structure with components important for language planning (*27*).

While regions of cMFG are known to be important for several non-linguistic functions, such as generating eye movements (*44*, *45*) (e.g., Fig. 1G), processing auditory information during motor tasks (*66*), cognitive control (*67–69*), and hand-related motor learning (*70*), its relation to language has remained unclear. Past DES mapping studies have reported that speech arrest and errors can result from cMFG perturbation, but these effects occur less regularly than from stimulation of cIFG and other frontotemporal structures (*8*, *9*, *11*, *24*); consequently, neurosurgical investigation of frontal language circuitry has largely focused on IFG and speech motor cortex (*13*, *18*, *23*, *40*,

41, *54*, *57*, *58*, *71*). However, recent studies have begun to indicate cMFG performs functions relevant to speech. For example, a large-scale imaging study identified a subregion of cMFG and adjacent precentral gyrus, referred to as Area 55b, that displays activity during linguistic tasks and exhibits strong connectivity to language-related circuitry (*72*). Likewise, cases of cMFG resection leading to transient (*6*) and long-lasting (*5*) deficits in verbal fluency have been reported. Our present stimulation results extend these important initial findings by demonstrating that cMFG is critically involved in the planning of spoken language – a conclusion which is further supported by our intracranial recordings of speech-selective preparatory activity in this area (*27*). Additional research is required to determine the exact planning operations (*73–75*) performed in cMFG and define the boundaries of its language-related territory, but its connections and close proximity to speech areas in cIFG (*72*, *76*), dorsal laryngeal motor cortex (*17*, *18*), and middle precentral gyrus (*56*) further motivate this region as a key node within the human language network.

Our broad sampling of the brain with DES and targeted measurement of RT revealed four sites where cortical stimulation resulted in significantly faster participant responses (fig. S5). Previous studies have reported that perturbation of cortical structures can improve or speed up task behavior in humans and animal models, suggesting that this phenomenon is generalizable across species and behaviors (*77*, *78*). For example, a focal cooling study in neurosurgical patients reported that speech rate could either increase or decrease when language-related premotor regions were cooled (*79*). We found that several sites outside of regions related to action and speech elicited faster responses; therefore, disrupting neural activity via DES may have modulated a variety of distinct processes both related and unrelated to language – such as global arousal, impulsivity, planning, and/or language comprehension – which ultimately led to faster RT. While the underlying mechanisms remain unknown, these data provide promising initial evidence for cortical stimulation as a therapy for augmenting cognitive function, perhaps in a manner analogous to the usage of deep brain stimulation and transcranial magnetic stimulation to treat motor and nonmotor symptoms in a range of disorders (*80–82*).

In conclusion, this study advances our understanding of the human language network by establishing cMFG as a critical speech-related planning area and confirming that cIFG causally contributes to the preparation of spoken language. Our results suggest these regions contribute to generating the meaning of speech (e.g., conceptual or lexical content) rather than its lower-level structure (e.g., phonological or phonetic content), as perturbing these regions elicited both slower RT and high-level errors (i.e., semantic paraphasia, hesitations, anomia) but not neologisms or articulatory errors. Therefore, cIFG and cMFG likely function as a key module in a larger network of both language-specific circuitry, such as those involved in encoding phonological form (*4*, *30*, *31*, *56*, *74*), as well as areas involved in general task performance (*55*, *61*, *62*) – for example, the longer RTs resulting from posterior cingulate stimulation (fig. S4) may have resulted from disrupted cognitive control (*83*, *84*). Further DES research combined with structured behavioral tasks is well-suited to identify additional components of this planning network and to delineate their precise contributions to typical and atypical language generation (*85–87*).

ACKNOWLEDGMENTS

Non-Author Contributions

We thank members of the Long laboratory as well as Taylor Abel, Frank Guenther, Elnaz Hozhabri, Jelena Krivokapić, Kenway Louie, Felix Moll, Caroline Niziolek, and Shy Shoham for comments on earlier versions of this manuscript. We also thank Joel Berger, Haiming Chen, Phillip Gander, Christopher Garcia, Matthew Howard III, My Hieu Kien Huynh, Kenji Ibayashi, Zahra Jourahmad, Hiroto Kawasaki, Mac McKay, Kirill Nourski, Ariane Rhone, and Andrea Rohl for help with data collection, and we also acknowledge helpful conversations with Frank Guenther and Jelena Krivokapić.

Funding

This research was supported by R01 DC019354 (M.A.L.), R01 DC015260 (J.D.W.G.), and Simons Collaboration on the Global Brain (M.A.L.).

Author Contributions

G.A.C. and M.A.L. conceived the study and designed the experiments; G.A.C., D.C., and J.D.W.G. conducted the research; G.A.C., C.K.K., F.T., D.C., and M.A.L. performed data analyses; G.A.C. and M.A.L. created the Figures; G.A.C. wrote the initial draft of the manuscript; G.A.C., C.K.K., F.T., D.C., J.D.W.G., and M.A.L edited and reviewed the final manuscript. J.D.W.G. and M.A.L acquired funding; J.D.W.G. and M.A.L. supervised the project.

Competing Interests

The authors declare no competing interests.

Data and Availability

The corresponding author will provide all analysis code and deidentified behavioral data upon request.

LIST OF SUPPLEMENTARY MATERIALS

Materials and Methods
Figures S1 to S5
Tables S1 and S2
References (*1-11*)

REFERENCES

1. S. C. Levinson, F. Torreira, Timing in turn-taking and its implications for processing models of language. *Front. Psychol.* **6** (2015), doi:10.3389/fpsyg.2015.00731.
2. G. A. Castellucci, F. H. Guenther, M. A. Long, A Theoretical Framework for Human and Nonhuman Vocal Interaction. *Annu. Rev. Neurosci.* **45**, 295–316 (2022).
3. N. F. Dronkers, O. Plaisant, M. T. Iba-Zizen, E. A. Cabanis, Paul Broca's historic cases: high resolution MR imaging of the brains of Leborgne and Lelong. *Brain*. **130**, 1432–1441 (2007).
4. D. Mirman, A. E. Kraft, D. Y. Harvey, A. R. Brecher, M. F. Schwartz, Mapping articulatory and grammatical subcomponents of fluency deficits in post-stroke aphasia. *Cogn. Affect. Behav. Neurosci.* **19**, 1286–1298 (2019).
5. E. F. Chang, G. Kurteff, J. P. Andrews, R. G. Briggs, A. K. Conner, J. D. Battiste, M. E. Sughrue, Pure Apraxia of Speech After Resection Based in the Posterior Middle Frontal Gyrus. *Neurosurgery*. **87**, E383–E389 (2020).
6. R. A. Morshed, A. T. Lee, E. J. Wang, J. S. Young, S. Cha, S. L. Hervey-Jumper, M. S. Berger, Functional outcomes after resection of middle frontal gyrus diffuse gliomas. *J. Neurosurg.* **137**, 1–8 (2022).
7. K. J. Forseth, C. M. Kadipasaoglu, C. R. Conner, G. Hickok, R. T. Knight, N. Tandon, A lexical semantic hub for heteromodal naming in middle fusiform gyrus. *Brain*. **141**, 2112–2126 (2018).
8. E. F. Chang, J. D. Breshears, K. P. Raygor, D. Lau, A. M. Molinaro, M. S. Berger, Stereotactic probability and variability of speech arrest and anomia sites during stimulation mapping of the language dominant hemisphere. *J. Neurosurg.* **126**, 114–121 (2017).
9. M. C. Tate, G. Herbet, S. Moritz-Gasser, J. E. Tate, H. Duffau, Probabilistic map of critical functional regions of the human cerebral cortex: Broca's area revisited. *Brain*. **137**, 2773–2782 (2014).
10. W. Penfield, E. Boldrey, SOMATIC MOTOR AND SENSORY REPRESENTATION IN THE CEREBRAL CORTEX OF MAN AS STUDIED BY ELECTRICAL STIMULATION. *Brain*. **60**, 389–443 (1937).
11. W. Penfield, L. Roberts, "THE EVIDENCE FROM CORTICAL MAPPING" in *Speech and Brain Mechanisms* (Princeton University Press, 1959), pp. 119–137.
12. B. L. Chernoff, M. H. Sims, S. O. Smith, W. H. Pilcher, B. Z. Mahon, Direct electrical stimulation of the left frontal aslant tract disrupts sentence planning without affecting articulation. *Cogn. Neuropsychol.* **36**, 178–192 (2019).
13. J. D. Breshears, A. M. Molinaro, E. F. Chang, A probabilistic map of the human ventral sensorimotor cortex using electrical stimulation. *J. Neurosurg.* **123**, 340–349 (2015).
14. G. Ojemann, J. Ojemann, E. Lettich, M. Berger, Cortical language localization in left, dominant hemisphere. *J Neurosurg*. **71** (1989).
15. H. Duffau, The role of dominant premotor cortex in language: a study using intraoperative functional mapping in awake patients. *NeuroImage*. **20**, 1903–1914 (2003).
16. L. Schaffler, H. O. Luders, G. J. Beck, Quantitative Comparison of Language Deficits Produced by Extraoperative Electrical Stimulation of Broca's, Wernicke's, and Basal Temporal Language Areas. *Epilepsia*. **37**, 463–475 (1996).
17. J. R. Belkhir, W. T. Fitch, F. E. Garcea, B. L. Chernoff, M. H. Sims, E. Navarrete, S. Haber, D. A. Paul, S. O. Smith, W. H. Pilcher, B. Z. Mahon, Direct electrical stimulation evidence for a dorsal motor area with control of the larynx. *Brain Stimulat.* **14**, 110–112 (2021).
18. B. K. Dichter, J. D. Breshears, M. K. Leonard, E. F. Chang, The Control of Vocal Pitch in Human Laryngeal Motor Cortex. *Cell*. **174**, 21-31.e9 (2018).
19. F. W. Moll, D. Kranz, A. Corredera Asensio, M. Elmaleh, L. A. Ackert-Smith, M. A. Long, Thalamus drives vocal onsets in the zebra finch courtship song. *Nature*. **616**, 132–136 (2023).
20. D. E. Okobi, A. Banerjee, A. M. M. Matheson, S. M. Phelps, M. A. Long, Motor cortical control of vocal interaction in neotropical singing mice. *Science*. **363**, 983–988 (2019).
21. F. Caruana, A. Jezzini, B. Sbriscia-Fioretti, G. Rizzolatti, V. Gallese, Emotional and Social Behaviors Elicited by Electrical Stimulation of the Insula in the Macaque Monkey. *Curr. Biol.* **21**, 195–199 (2011).
22. Y. Yajima, Y. Hayashi, N. Yoshi, The midbrain central gray substance as a highly sensitive neural structure for the production of ultrasonic vocalization in the rat. *Brain Res.* **198**, 446–452 (1980).
23. J. D. Breshears, D. G. Southwell, E. F. Chang, Inhibition of Manual Movements at Speech Arrest Sites in the Posterior Inferior Frontal Lobe. *Neurosurgery*. **85**, E496–E501 (2019).

24. N. Sanai, Z. Mirzadeh, M. S. Berger, Functional Outcome after Language Mapping for Glioma Resection. *N. Engl. J. Med.*, 10 (2008).
25. K. J. Forseth, G. Hickok, P. S. Rollo, N. Tandon, Language prediction mechanisms in human auditory cortex. *Nat. Commun.* **11**, 5240 (2020).
26. J. G. Ojemann, G. A. Ojemann, E. Lettich, Cortical stimulation mapping of language cortex by using a verb generation task: effects of learning and comparison to mapping based on object naming. *J. Neurosurg.* **97**, 33–38 (2002).
27. G. A. Castellucci, C. K. Kovach, M. A. Howard, J. D. W. Greenlee, M. A. Long, A speech planning network for interactive language use. *Nature*. **602**, 117–122 (2022).
28. S. Bögels, L. Magyari, S. C. Levinson, Neural signatures of response planning occur midway through an incoming question in conversation. *Sci. Rep.* **5** (2015), doi:10.1038/srep12881.
29. S. Bögels, M. Casillas, S. C. Levinson, Planning versus comprehension in turn-taking: Fast responders show reduced anticipatory processing of the question. *Neuropsychologia*. **109**, 295–310 (2018).
30. P. Indefrey, The Spatial and Temporal Signatures of Word Production Components: A Critical Update. *Front. Psychol.* **2** (2011), doi:10.3389/fpsyg.2011.00255.
31. D. Kemmerer, From blueprints to brain maps: the status of the Lemma Model in cognitive neuroscience. *Lang. Cogn. Neurosci.* **34**, 1085–1116 (2019).
32. S. A. Kotz, A. D'Ausilio, T. Raettig, C. Begliomini, L. Craighero, M. Fabbri-Destro, C. Zingales, P. Haggard, L. Fadiga, Lexicality drives audio-motor transformations in Broca's area. *Brain Lang.* **112**, 3–11 (2010).
33. C. Rogalsky, G. Hickok, The Role of Broca's Area in Sentence Comprehension. **23**.
34. G. Hickok, D. Poeppel, The cortical organization of speech processing. *Nat. Rev. Neurosci.* **8**, 393–402 (2007).
35. V. Maffei, I. Indovina, E. Mazzarella, M. A. Giusti, E. Macaluso, F. Lacquaniti, P. Viviani, Sensitivity of occipito-temporal cortex, premotor and Broca's areas to visible speech gestures in a familiar language. *PLOS ONE*. **15**, e0234695 (2020).
36. R. Mukamel, Coupling Between Neuronal Firing, Field Potentials, and fMRI in Human Auditory Cortex. *Science*. **309**, 951–954 (2005).
37. K. V. Nourski, M. Steinschneider, A. E. Rhone, Electrocorticographic Activation within Human Auditory Cortex during Dialog-Based Language and Cognitive Testing. *Front. Hum. Neurosci.* **10** (2016), doi:10.3389/fnhum.2016.00202.
38. M. A. Howard, I. O. Volkov, R. Mirsky, P. C. Garell, M. D. Noh, M. Granner, H. Damasio, M. Steinschneider, R. A. Reale, J. E. Hind, J. F. Brugge, Auditory cortex on the human posterior superior temporal gyrus. *J. Comp. Neurol.* **416**, 79–92 (2000).
39. M. Keshishian, S. Akkol, J. Herrero, S. Bickel, A. D. Mehta, N. Mesgarani, Joint, distributed and hierarchically organized encoding of linguistic features in the human auditory cortex. *Nat. Hum. Behav.* (2023), doi:10.1038/s41562-023-01520-0.
40. K. E. Bouchard, N. Mesgarani, K. Johnson, E. F. Chang, Functional organization of human sensorimotor cortex for speech articulation. *Nature*. **495**, 327–332 (2013).
41. V. Ferpozzi, L. Fornia, M. Montagna, C. Siodambro, A. Castellano, P. Borroni, M. Riva, M. Rossi, F. Pessina, L. Bello, G. Cerri, Broca's Area as a Pre-articulatory Phonetic Encoder: Gating the Motor Program. *Front. Hum. Neurosci.* **12**, 64 (2018).
42. E. Bates, S. D'Amico, T. Jacobsen, A. Székely, E. Andonova, A. Devescovi, D. Herron, C. Ching Lu, T. Pechmann, C. Pléh, N. Wicha, K. Federmeier, I. Gerdjikova, G. Gutierrez, D. Hung, J. Hsu, G. Iyer, K. Kohnert, T. Mehotcheva, A. Orozco-Figueroa, A. Tzeng, O. Tzeng, Timed picture naming in seven languages. *Psychon. Bull. Rev.* **10**, 344–380 (2003).
43. S. C. Levinson, F. Torreira, Timing in turn-taking and its implications for processing models of language. *Front. Psychol.* **6** (2015), doi:10.3389/fpsyg.2015.00731.
44. E. Lobel, P. Kahane, U. Leonards, M.-H. Grosbras, S. Lehéricy, D. L. Bihan, A. Berthoz, Localization of human frontal eye fields: anatomical and functional findings of functional magnetic resonance imaging and intracerebral electrical stimulation. *J. Neurosurg.* **95**, 804–815 (2001).
45. C. Amiez, M. Petrides, Anatomical organization of the eye fields in the human and non-human primate frontal cortex. *Prog. Neurobiol.* **89**, 220–230 (2009).
46. E. M. Gordon, R. J. Chauvin, A. N. Van, A. Rajesh, A. Nielsen, D. J. Newbold, C. J. Lynch, N. A. Seider, S. R. Krimmel, K. M. Scheidter, J. Monk, R. L. Miller, A. Metoki, D. F. Montez, A. Zheng, I. Elbau, T. Madison, T. Nishino, M. J. Myers, S. Kaplan, C. Badke D'Andrea, D. V. Demeter, M. Feigelis, J. S. B. Ramirez, T. Xu, D. M. Barch, C. D. Smyser, C. E. Rogers, J. Zimmermann, K. N. Botteron, J. R. Pruett, J. T.

Willie, P. Brunner, J. S. Shimony, B. P. Kay, S. Marek, S. A. Norris, C. Gratton, C. M. Sylvester, J. D. Power, C. Liston, D. J. Greene, J. L. Roland, S. E. Petersen, M. E. Raichle, T. O. Laumann, D. A. Fair, N. U. F. Dosenbach, A somato-cognitive action network alternates with effector regions in motor cortex. *Nature* (2023), doi:10.1038/s41586-023-05964-2.

47. M. H. Histed, V. Bonin, R. C. Reid, Direct Activation of Sparse, Distributed Populations of Cortical Neurons by Electrical Microstimulation. *Neuron*. **63**, 508–522 (2009).
48. E. Seidemann, A. Arieli, A. Grinvald, H. Slovin, Dynamics of Depolarization and Hyperpolarization in the Frontal Cortex and Saccade Goal. *Science*. **295**, 862–865 (2002).
49. H. Lüders, R. P. Lesser, J. Hahn, D. S. Dinner, H. H. Morris, E. Wyllie, J. Godoy, BASAL TEMPORAL LANGUAGE AREA. *Brain*. **114**, 743–754 (1991).
50. J. R. Binder, J. Tong, S. B. Pillay, L. L. Conant, C. J. Humphries, M. Raghavan, W. M. Mueller, R. M. Busch, L. Allen, W. L. Gross, C. T. Anderson, C. E. Carlson, M. J. Lowe, J. T. Langfitt, M. E. Tivarus, D. L. Drane, D. W. Loring, M. Jacobs, V. L. Morgan, J. B. Allendorfer, J. P. Szaflarski, L. Bonilha, S. Bookheimer, T. Grabowski, J. Vannest, S. J. Swanson, fMRI in Anterior Temporal Epilepsy Surgery (FATES) study, Temporal lobe regions essential for preserved picture naming after left temporal epilepsy surgery. *Epilepsia*. **61**, 1939–1948 (2020).
51. S. T. Klapp, D. Maslovat, Programming of action timing cannot be completed until immediately prior to initiation of the response to be controlled. *Psychon. Bull. Rev.* (2020), doi:10.3758/s13423-020-01740-9.
52. H. S. Z. Wynne, L. Wheeldon, A. Lahiri, Compounds, phrases and clitics in connected speech. *J. Mem. Lang.* **98**, 45–58 (2018).
53. M. Heldner, J. Edlund, Pauses, gaps and overlaps in conversations. *J. Phon.* **38**, 555–568 (2010).
54. E. F. Chang, G. Kurteff, S. M. Wilson, Selective Interference with Syntactic Encoding during Sentence Production by Direct Electrocortical Stimulation of the Inferior Frontal Gyrus. *J. Cogn. Neurosci.* **30**, 411–420 (2018).
55. A. Basilakos, K. G. Smith, P. Fillmore, J. Fridriksson, E. Fedorenko, Functional Characterization of the Human Speech Articulation Network. *Cereb. Cortex*. **28**, 1816–1830 (2018).
56. A. B. Silva, J. R. Liu, L. Zhao, D. F. Levy, T. L. Scott, E. F. Chang, A Neurosurgical Functional Dissection of the Middle Precentral Gyrus during Speech Production. *J. Neurosci.* **42**, 8416–8426 (2022).
57. A. Flinker, A. Korzeniewska, A. Y. Shestyuk, P. J. Franaszczuk, N. F. Dronkers, R. T. Knight, N. E. Crone, Redefining the role of Broca's area in speech. *Proc Natl Acad Sci U A*. **112**, 2871–5 (2015).
58. N. T. Sahin, S. Pinker, S. S. Cash, D. Schomer, E. Halgren, Sequential Processing of Lexical, Grammatical, and Phonological Information Within Broca's Area. *Science*. **326**, 445–449 (2009).
59. M. Papoutsi, J. A. de Zwart, J. M. Jansma, M. J. Pickering, J. A. Bednar, B. Horwitz, From Phonemes to Articulatory Codes: An fMRI Study of the Role of Broca's Area in Speech Production. *Cereb. Cortex*. **19**, 2156–2165 (2009).
60. Y. Grodzinsky, A. Santi, The battle for Broca's region. *Trends Cogn. Sci.* **12**, 474–480 (2008).
61. E. Fedorenko, J. Duncan, N. Kanwisher, Language-Selective and Domain-General Regions Lie Side by Side within Broca's Area. *Curr. Biol.* **22**, 2059–2062 (2012).
62. J. M. Novick, J. C. Trueswell, S. L. Thompson-Schill, Broca's Area and Language Processing: Evidence for the Cognitive Control Connection: Broca's Area and Language Processing. *Lang. Linguist. Compass*. **4**, 906–924 (2010).
63. P. Tremblay, A. S. Dick, Broca and Wernicke are dead, or moving past the classic model of language neurobiology. *Brain Lang.* **162**, 60–71 (2016).
64. H. Duffau, The error of Broca: From the traditional localizationist concept to a connectomal anatomy of human brain. *J. Chem. Neuroanat.* **89**, 73–81 (2018).
65. E. Fedorenko, I. A. Blank, Broca's Area Is Not a Natural Kind. *Trends Cogn. Sci.* **24**, 270–284 (2020).
66. T. Hosman, J. B. Hynes, J. Saab, K. G. Wilcoxen, B. R. Buchbinder, N. Schmansky, S. S. Cash, E. N. Eskandar, J. D. Simeral, B. Franco, J. Kelemen, C. E. Vargas-Irwin, L. R. Hochberg, Auditory cues reveal intended movement information in middle frontal gyrus neuronal ensemble activity of a person with tetraplegia. *Sci. Rep.* **11**, 98 (2021).
67. B. R. Buchsbaum, S. Greer, W.-L. Chang, K. F. Berman, Meta-analysis of neuroimaging studies of the Wisconsin Card-Sorting task and component processes. *Hum. Brain Mapp.* **25**, 35–45 (2005).
68. J. Sierpowska, A. Fernandez-Coello, A. Gomez-Andres, À. Camins, S. Castañer, M. Juncadella, A. Gabarrós, A. Rodríguez-Fornells, Involvement of the middle frontal gyrus in language switching as revealed by electrical stimulation mapping and functional magnetic resonance imaging in bilingual brain tumor patients. *Cortex*. **99**, 78–92 (2018).

69. M. Brass, The Role of the Frontal Cortex in Task Preparation. *Cereb. Cortex*. **12**, 908–914 (2002).
70. N. Kumar, A. Sidarta, C. Smith, D. J. Ostry, *eneuro*, in press, doi:10.1523/ENEURO.0269-22.2022.
71. E. M. Mugler, M. C. Tate, K. Livescu, J. W. Templer, M. A. Goldrick, M. W. Slutzky, Differential Representation of Articulatory Gestures and Phonemes in Precentral and Inferior Frontal Gyri. *J. Neurosci.* **38**, 9803–9813 (2018).
72. M. F. Glasser, T. S. Coalson, E. C. Robinson, C. D. Hacker, J. Harwell, E. Yacoub, K. Ugurbil, J. Andersson, C. F. Beckmann, M. Jenkinson, S. M. Smith, D. C. Van Essen, A multi-modal parcellation of human cerebral cortex. *Nature*. **536**, 171–178 (2016).
73. P. Indefrey, W. J. M. Levelt, The spatial and temporal signatures of word production components. *Cognition*. **92**, 101–144 (2004).
74. Guenther, Frank H., *Neural Control of Speech* (MIT Press, 2016).
75. G. S. Dell, A spreading-activation theory of retrieval in sentence production. *Psychol. Rev.* **93**, 283–321 (1986).
76. M. Catani, F. Dell'Acqua, F. Vergani, F. Malik, H. Hodge, P. Roy, R. Valabregue, M. Thiebaut de Schotten, Short frontal lobe connections of the human brain. *Cortex*. **48**, 273–291 (2012).
77. E. Zagha, X. Ge, D. A. McCormick, Competing Neural Ensembles in Motor Cortex Gate Goal-Directed Motor Output. *Neuron*. **88**, 565–577 (2015).
78. R. Guzulaitis, L. Godenzini, L. M. Palmer, Neural basis of anticipation and premature impulsive action in the frontal cortex. *Nat. Neurosci.* **25**, 1683–1692 (2022).
79. M. A. Long, K. A. Katlowitz, M. A. Svirsky, R. C. Clary, T. M. Byun, N. Majaj, H. Oya, M. A. Howard, J. D. W. Greenlee, Functional Segregation of Cortical Regions Underlying Speech Timing and Articulation. *Neuron*. **89**, 1187–1193 (2016).
80. A. M. Lozano, N. Lipsman, H. Bergman, P. Brown, S. Chabardes, J. W. Chang, K. Matthews, C. C. McIntyre, T. E. Schlaepfer, M. Schulder, Y. Temel, J. Volkmann, J. K. Krauss, Deep brain stimulation: current challenges and future directions. *Nat. Rev. Neurol.* **15**, 148–160 (2019).
81. J. Reis, H. M. Schambra, L. G. Cohen, E. R. Buch, B. Fritsch, E. Zarahn, P. A. Celnik, J. W. Krakauer, Noninvasive cortical stimulation enhances motor skill acquisition over multiple days through an effect on consolidation. *Proc. Natl. Acad. Sci.* **106**, 1590–1595 (2009).
82. L. De Risio, M. Borgi, M. Pettorruso, A. Miuli, A. M. Ottomana, A. Sociali, G. Martinotti, G. Nicolò, S. Macrì, M. Di Giannantonio, F. Zoratto, Recovering from depression with repetitive transcranial magnetic stimulation (rTMS): a systematic review and meta-analysis of preclinical studies. *Transl. Psychiatry*. **10**, 393 (2020).
83. R. Leech, R. Braga, D. J. Sharp, Echoes of the Brain within the Posterior Cingulate Cortex. *J. Neurosci.* **32**, 215–222 (2012).
84. J. M. Pearson, B. Y. Hayden, S. Raghavachari, M. L. Platt, Neurons in Posterior Cingulate Cortex Signal Exploratory Decisions in a Dynamic Multioption Choice Task. *Curr. Biol.* **19**, 1532–1537 (2009).
85. K. Deger, W. Ziegler, Speech motor programming in apraxia of speech. *J. Phon.* **30**, 321–335 (2002).
86. E. S. Jackson, S. Wijeakumar, D. S. Beal, B. Brown, P. Zebrowski, J. P. Spencer, A fNIRS Investigation of Speech Planning and Execution in Adults Who Stutter. *Neuroscience*. **406**, 73–85 (2019).
87. A. Whillier, S. Hommel, N. E. Neef, A. Wolff von Gudenberg, W. Paulus, M. Sommer, Adults who stutter lack the specialised pre-speech facilitation found in non-stutterers. *PLOS ONE*. **13**, e0202634 (2018).

MATERIALS AND METHODS

Participants

Study participants were patient-volunteers undergoing surgical treatment at the University of Iowa Hospitals and Clinics for medically intractable epilepsy, brain tumors, or implantation of deep brain stimulation (DBS) electrodes. Data from participants with previous brain resections or infarcts were not included in this study. During the course of their treatment, participants were implanted either with electrocorticography (ECoG) and/or intracerebral stereo-EEG depth (sEEG) electrodes for seizure focus determination, underwent a clinically required awake craniotomy, or underwent awake DBS lead implantation. In ten participants, language function was confirmed to be either left lateralized or bihemispherically distributed using Wada testing or functional magnetic resonance imaging; the remaining participants were right-handed (n = 11) or left-handed (n = 2) with unknown lateralization for language. All participants consented to participate in research, and the University of Iowa Institutional Review Board approved all research procedures. Finally, all participants were native speakers of English except for one (684L), who was a native speaker of Vietnamese; consequently, this participant was only screened for stimulation-induced sensorimotor effects and their behavioral data were not analyzed further. Additional demographic and clinical information is available in table S1.

Data Acquisition

For awake craniotomy patients, electrical signals resulting from direct electrical stimulation (DES) were recorded using subdural ECoG grids and/or strips manufactured by Ad-Tech Medical or PMT. Signals were amplified and sampled at 2034.5 Hz using a multichannel amplifier and digital acquisition system (PZ2 or PZ5 preamplifier with an RZ2 processer; Tucker-Davis Technologies). For chronically implanted epilepsy patients, electrical signals from subdural electrode grids, strips, or sEEG intracerebral depth electrodes (AdTech) were recorded at 2000 Hz with a multichannel amplifier and digital acquisition system (Atlas system, Neuralynx). In both contexts, analog input channels synchronized with the neural recordings additionally acquired the output of 1-3 microphone(s) which captured the speech acoustics of the experimenter and participant. Input channels were typically sampled at 48,828 Hz by the TDT system and 16,000 Hz by the Neuralynx system and downsampled offline. In addition to the electrical signals, a video of the participant was also acquired at 24 fps for 20 of 23 experiments. The video was synced to the electrophysiological data after the experiment and provided a secondary high-quality audio recording channel of the experiment, which was sampled at 48 kHz.

In a single awake craniotomy experiment, electrical signals were not recorded due to a recording system error and consequently only a video of the experiment was recorded (641L; see table S1). This video provided images of the stimulator and captured experiment acoustics; thus, stimulation and behavioral timing was estimated using this data stream.

Direct Electrical Stimulation (DES)

DES was performed using a constant voltage stimulator (SD9, Grass Instruments). Charge balanced, biphasic pulses (0.2 ms duration) at 50 Hz were applied to the brain using either: 1) a handheld stimulator (Magstim BiPolar Probe; MVAP Medical Supplies, Inc., Thousand Oaks, CA) in awake craniotomy for tumor resection, 2) subdural ECoG strip electrodes (AdTech) in awake craniotomies for deep brain stimulator implantation, or 3) subdural ECoG grid/strip electrodes or sEEG electrodes (AdTech) in chronic epilepsy monitoring procedures. Because the position of the

handheld stimulator could vary slightly from trial to trial (e.g., the stimulator could be removed momentarily to apply saline to the brain), we considered stimulation locations that varied by less than a centimeter to represent a single stimulation site. To titrate the stimulation voltage level, DES was first applied starting at ~5V and increased in ~2.5V steps until the participant reported a sensation, after-discharges were observed, or a maximum of 20-25V was reached. The highest voltage not resulting in a sensation or after-discharges was used as the stimulation level for the experiment. Occasionally, the stimulation voltage would be lowered during the course of an experiment if delayed after-discharges were observed. The stimulation voltage at each site included for analysis in this study is reported in table S2; in cases where the voltage was lowered, the lowest intensity is reported.

Stimulation timing was manually controlled by the experimenter, who also presented the questions to the participant in most cases – however, in some experiments, a separate experimenter presented questions and another delivered stimulation. The experimenter controlling the stimulator typically began applying DES prior to CI presentation and stopped when the participant spoke their response. However, considerable variability in stimulation timing was observed across trials, and any trial where DES was applied between CI offset and answer onset was considered a 'stimulated' trial. In all cases, participants could not see or hear when the stimulation was delivered by the experimenter.

Anatomical Reconstructions

Cortical surface reconstruction was performed using T1-weighted or magnetization-prepared rapid gradient-echo (MPRAGE) images obtained during the clinical workup and the 'recon-all' pipeline in FreeSurfer (*1*). In cases of poor T1 imaging, FreeSurfer processing was repeated with combined T1 and T2 images or T1 images with fluid-attenuated inversion recovery (FLAIR) sequences to improve pial surface parcellation. White-matter segmentation errors resulting from low image quality or tissue abnormalities were corrected manually.

Stimulation site localization in awake craniotomies for tumor resection

In one intraoperative tumor resection case (494L), stimulation site localization and coregistration was performed using intraoperative photographs, which were aligned to reconstructed cortical surface meshes via visual comparison of gyral anatomy by two raters (G.A.C. and J.D.W.G.). In all other cases, intraoperative photographs along with pre- and postoperative magnetic resonance (MR) images were used to localize both heads of the hand-held stimulator probe. To precisely localize the craniotomy, we first 1) aligned intraoperative photographs to reconstructed cortical surfaces via visual inspection, 2) coregistered any burr holes and bone flap margins visible on the postoperative MR images to preoperative images using the FLIRT tool in the FSL package (*2*), and 3) recorded the coordinates from the Stealth neuro-navigation system (Medtronic, Minneapolis, MN, USA) used for craniotomy planning. Stimulation position was then defined on cortical surface renderings via visual comparison of gyral anatomy by two independent raters (F.T. and C.K.K) and cross-verification with a third rater (J.D.W.G.).

Electrode localization in awake craniotomies for deep brain stimulator implantations

Localization of subdural ECoG strip electrodes (Ad-Tech, Racine, WI, USA) in patients undergoing deep brain stimulation (DBS) surgery was performed using a combination of intraoperative fluoroscopy, preoperative MR images, and pre- and post-implantation computed

tomography (CT) collected for clinical reasons. Because the ECoG strips were temporarily placed during surgery and removed before closure, intraoperative fluoroscopy was required to record strip locations for surface-based localization while CT and MR images were used to reconstruct cortical surfaces and align the fluoroscopic images. First, all MR and CT images were converted from DICOM (Digital Imaging and Communications in Medicine) to NIfTI (Neuroimaging Informatics Technology Initiative) format using dsm2niix tool in MRIcroGL (*3*). Preoperative CT scans were then employed as a 3D frame for the coregistration of 2D fluoroscopic images. Specifically, the 'isosurface' function in MATLAB was used to compute the surface geometry of the preoperative CT, and cortical surface meshes were then transformed into CT space. To coregister the fluoroscopic image, multiple common control points were identified in the CT volume and 2D fluoroscopic projection. Control points included skull contours, the superior and inferior terminations of the frontal sinuses, the glabella, screws of the stereotactic frame (CRW; Integra, Inc., Princeton, NJ). Because the view plane angle and field of view varied between fluorograms, control points were individualized based on the visible skull anatomy. For each individual, a minimum of four different control points were utilized. For cases with an insufficient number of plainly visible skull landmarks, a post-implantation CT which displayed DBS leads and burr hole covers was coregistered with the pre-implantation CT to provide an additional set of reference points. Next, an orthographic projection from the CT image space to the imaging plane of the fluoroscope was computed through constrained minimization of squared error between control points. This procedure yielded an orthogonal affine projection relating control points in CT space to those in the fluorograms. After this alignment, ECoG electrode locations were defined as the point at which a line orthogonal to the fluoroscopy-aligned view plain, passing through the electrode shadow visible in the fluorogram, intersected the cortical surface. Finally, the RAS coordinates of each electrode were transferred to Montreal Neurological Institute (MNI) space.

Electrode localization in chronically implanted patients

Electrode localization in epilepsy patients undergoing chronic electrode implantation was performed by identifying characteristic metallic-induced susceptibility artifacts and punctuate radiodensities in post-implantation MR and CT images, respectively. Electrode coordinates were then transferred to pre-implantation images via linear image coregistration, followed by manually guided thin-plate spline (TPS) warping to account for nonlinear imaging and structural distortions. Control points for TPS warping were determined by visually identifying corresponding landmark coordinates in pre- and post-implantation imaging.

Stimulation site coregistration

All contact locations were first determined on cortical surface renderings in Right-Anterior-Superior (RAS) coordinate space. Anatomical labelling of the electrodes was performed through surface-based coregistration and segmentation for each participant using the Desikan-Killiany-Tourville (DKT) atlas (*4*, *5*) as assigned by FreeSurfer (*6*). After automatic parcellation, electrode locations relative to DKT atlas labels were visually inspected by two raters (G.A.C and J.D.W.G) and corrected if necessary. To provide a consistent operational boundary between rostral and caudal middle frontal gyrus in line with our previous research (*7*), raters considered any stimulation sites posterior to the extension of the anterior horizontal ramus of the inferior frontal gyrus as within caudal middle frontal gyrus and those anterior to this point to be within rostral middle frontal gyrus. Finally, preoperative T1 images were non-linearly coregistered to an MNI-aligned

template brain (CIT168 template) (*8*) using symmetric diffeomorphic registration in the ANTs toolbox (*9*) to transfer electrode locations to MNI space.

Stimulation sites on the lateral cortical surface and superior temporal plane in individual participants were rendered on coregistration plots (e.g., Fig. 1b) by plotting the center of the two stimulation electrodes on the gyral surface of the MNI152 reference brain. The locations of sEEG stimulation sites were rendered on canonical and individual cortical surfaces by plotting the coregistered coordinates of the most superficial contact of the electrode shaft on the gyral surface of the MNI152 brain or the location where the shaft penetrated the gyral surface, respectively. SEEG stimulation sites located on the medial cortical surface, within insular cortex, or on the ventral cortical surface (i.e., "non-surface sites"; n = 6) were not rendered on coregistration plots. The coordinates for each pair of stimulated electrodes are reported table S2.

Behavioral Task

Participants completed the Critical Information (CI) task, which required participants to answer simple questions read aloud by an experimenter as quickly as possible. The CI questions were adapted from a stimulus set used in our previous work (*7*) that itself was adapted from an established Dutch stimulus set (*10*, *11*). Each CI question contains a single word (i.e., the critical information) which is required to answer the question (Fig. 1A). In most experiments, questions required participants to generate the antonym of common words; however, in a subset of experiments, questions could also ask about animal sounds or body parts.

Questions were presented either in randomized order or in pseudorandomized order to avoid repeating the same CI on subsequent trials. On approximately half of the trials, DES was applied. In most experiments, stimulated and control (i.e., non-stimulated) trials were balanced such that the same question would be presented twice – once as a control trial and once as a stimulated trial. However, because of clinical considerations (e.g., time constraints in the operating room, to avoid after-discharges), question order, stimulation status, and wording often deviated from the planned protocol. In addition, most participants completed a block of the CI questions prior to the stimulation experiment to familiarize them with the task; these data were not analyzed in the present study. In one participant (460L), other tasks (e.g., repeating syllables, pressing a button) were often interleaved with trials of the CI task.

The audio acquired with the electrophysiological acquisition system and/or video camera was annotated and timestamped by a trained phonetician (G.A.C.) to determine the onsets and offsets of all experimenter questions, CI, and participant responses. All final timestamping was performed blind in regard to stimulation timing. Questions which could not be accurately timestamped due to background noise (e.g., clinical team talking in background, operating room door closing, medical instrument alerts) were excluded from analysis. Likewise, any antonym question where the participant gave an answer using "not" and the CI (e.g., Question: The opposite of hungry is what word? Answer: Not hungry) were rejected to ensure participants performed the task by generating a lexical item rather than repeating the CI. Aside from correct answers, any of the following were noted:

> <u>Semantic paraphasia</u>: 1) an incorrect answer (i.e., giving a synonym when the question required an antonym or giving an answer unrelated semantically to the CI) to a question

which was answered correctly at least once (e.g., Question: Which word is the opposite of fast? Answer: "Rapid."; Question: "The opposite of hot is what common word?" Answer: "Two") or 2) answers related semantically to the CI and/or correct response were considered errors if the same correct answer at least twice during the experiment (e.g. Question: "The opposite of hungry is what familiar word?" Answer "Thirsty" would be considered an error only if "Full" or another correct answer were produced at least twice during the experiment). In both cases, an answer would be considered a semantic error if the participant spontaneously corrected their answer prior to completing the next trial (e.g., Fig. 2C), except when a participant offered additional correct responses.

Phonological paraphasia: a neologism, or an unattested English word consisting of segments that are properly articulated at a gross level.

Anomia: questions that the participant failed to answer or could not respond for any reason, except for trials where the participant either reported not being able to hear due to background noise or appeared to fall asleep, which were excluded from further analysis. The stimulation site in 494L (Fig. 1C,D) where perceptual dysfunction was reported was excluded from all analyses of anomia.

Hesitations: trials which the participant produced a hesitation (e.g., "uh", "um") or dysfluency (e.g., stuttering, repetition or prolongation of the first segment) prior to responding. In addition, because all CI questions could be answered with a single word, any answers where this word was preceded by filler words (e.g., Question: The opposite of hungry is what word? Answer: "The opposite of hungry is full.") were considered trials containing hesitations.

5) Qualitative results: any site where stimulation resulted in a sensory or motor effect (e.g., speech arrest, gaze deviation, dysarthria, etc.) as defined by a neurosurgeon (J.D.W.G.). Such effects were categorized as either 'speech sensorimotor' (i.e., speech arrest, orofacial tetanus, involuntary orofacial movement, orofacial sensation, dysarthria) or 'gaze sensorimotor' (i.e., involuntary head and/or eye movement). Any site which resulted in a sensation or movement that indicated the delivery of DES to the participant was not included in behavioral analyses. Descriptions of all qualitative sensorimotor results are provided in table S2.

Any site displaying a higher rate of semantic paraphasia, anomia, hesitations, and/or neologisms in stimulated versus control trials (minimum increase: 1%) was considered to display an increase in errors.

Behavioral Analysis

Reaction time (RT) was defined as the duration between question offset and answer onset (excluding any hesitations) and was computed for all trials performed (i.e., trials without anomia). Stimulus-response latency, defined as the duration between stimulation offset and answer onset, was calculated for all stimulated trials.

Stimulation-induced differences in RT at each site were assessed in early and late CI trials separately, as CI position significantly affects RT (*7*, *10*, *11*). Statistical significance in RT between control and stimulated trials was determined using a three-step process 1) rejecting outliers in the distributions of control and stimulated trials separately (i.e., any RT values greater than 2 interquartile ranges above the 75th percentile or less than 2 interquartile ranges below the 25th percentile), 2) identifying sites where the median RT in control and stimulated trials differed by at least 100 ms, and 3) performing rank-sum tests ($\alpha = 0.05$) on the outlier-rejected distributions of RT in control and stimulated trials. Behavioral analyses were not performed unless there were at least 8 performed stimulated and 8 performed control trials after outlier rejection. Due to restricted study times, we presented participants with more early trials than late trials (at an ~2:1 ratio); consequently, many sites did not have sufficient late trials for behavioral analysis. Trial numbers, RT summary statistics, and other behavioral data for each stimulation site is presented in table S2.

Statistical Analyses

All analyses, including permutation tests, were performed in MATLAB (Mathworks, Natick, MA) using custom-scripts. Rank-sum tests were performed with the 'ranksum' function, correlation analyses were performed with the 'corr' function, and logistic regression was performed using generalized linear modelling ('fitglm' function, with a binomial distribution, logit linkage function, and maximum of 1000 iterations specified). For all logistic regression analyses, the occurrence of stimulation-induced RT changes was used as the categorical response variable after excluding sites where DES evoked motor deficits; predictor variables were defined as follows:

1) Stimulation intensity vs. RT effect: Stimulation voltage was used as a single continuous predictor variable.
2) Clinical condition vs. RT effect: Stimulation sites were divided into three groups according to whether they were within participants treated for epilepsy, a brain tumor, or essential tremor/Parkinson's disease (combined due to limited sample size) (table S1). These groups were then used as categorical dummy variables, with the combined essential tremor/Parkinson's disease group designated as the reference category.
3) Stimulator type vs. RT effect: Stimulation sites were divided into three groups according to whether DES was delivered via ECoG electrodes, a handheld stimulator, or sEEG electrodes. These groups were then used as categorical dummy variables, with the sEEG group designated as the reference category.

REFERENCES

1. A. M. Dale, B. Fischl, M. I. Sereno, Cortical Surface-Based Analysis. *NeuroImage*. **9**, 179–194 (1999).
2. M. Jenkinson, P. Bannister, M. Brady, S. Smith, Improved Optimization for the Robust and Accurate Linear Registration and Motion Correction of Brain Images. *NeuroImage*. **17**, 825–841 (2002).
3. C. Rorden, M. Brett, Stereotaxic Display of Brain Lesions. *Behav. Neurol.* **12**, 191–200 (2000).
4. A. Klein, J. Tourville, 101 Labeled Brain Images and a Consistent Human Cortical Labeling Protocol. *Front. Neurosci.* **6** (2012), doi:10.3389/fnins.2012.00171.
5. R. S. Desikan, F. Ségonne, B. Fischl, B. T. Quinn, B. C. Dickerson, D. Blacker, R. L. Buckner, A. M. Dale, R. P. Maguire, B. T. Hyman, M. S. Albert, R. J. Killiany, An automated labeling system for subdividing the human cerebral cortex on MRI scans into gyral based regions of interest. *NeuroImage*. **31**, 968–980 (2006).
6. B. Fischl, Automatically Parcellating the Human Cerebral Cortex. *Cereb. Cortex*. **14**, 11–22 (2004).
7. G. A. Castellucci, C. K. Kovach, M. A. Howard, J. D. W. Greenlee, M. A. Long, A speech planning network for interactive language use. *Nature*. **602**, 117–122 (2022).
8. J. M. Tyszka, W. M. Pauli, In vivo delineation of subdivisions of the human amygdaloid complex in a high-resolution group template: In Vivo Amygdala Subdivisions. *Hum. Brain Mapp.* **37**, 3979–3998 (2016).
9. B. B. Avants, N. J. Tustison, G. Song, P. A. Cook, A. Klein, J. C. Gee, A reproducible evaluation of ANTs similarity metric performance in brain image registration. *NeuroImage*. **54**, 2033–2044 (2011).
10. S. Bögels, L. Magyari, S. C. Levinson, Neural signatures of response planning occur midway through an incoming question in conversation. *Sci. Rep.* **5** (2015), doi:10.1038/srep12881.
11. S. Bögels, M. Casillas, S. C. Levinson, Planning versus comprehension in turn-taking: Fast responders show reduced anticipatory processing of the question. *Neuropsychologia*. **109**, 295–310 (2018).

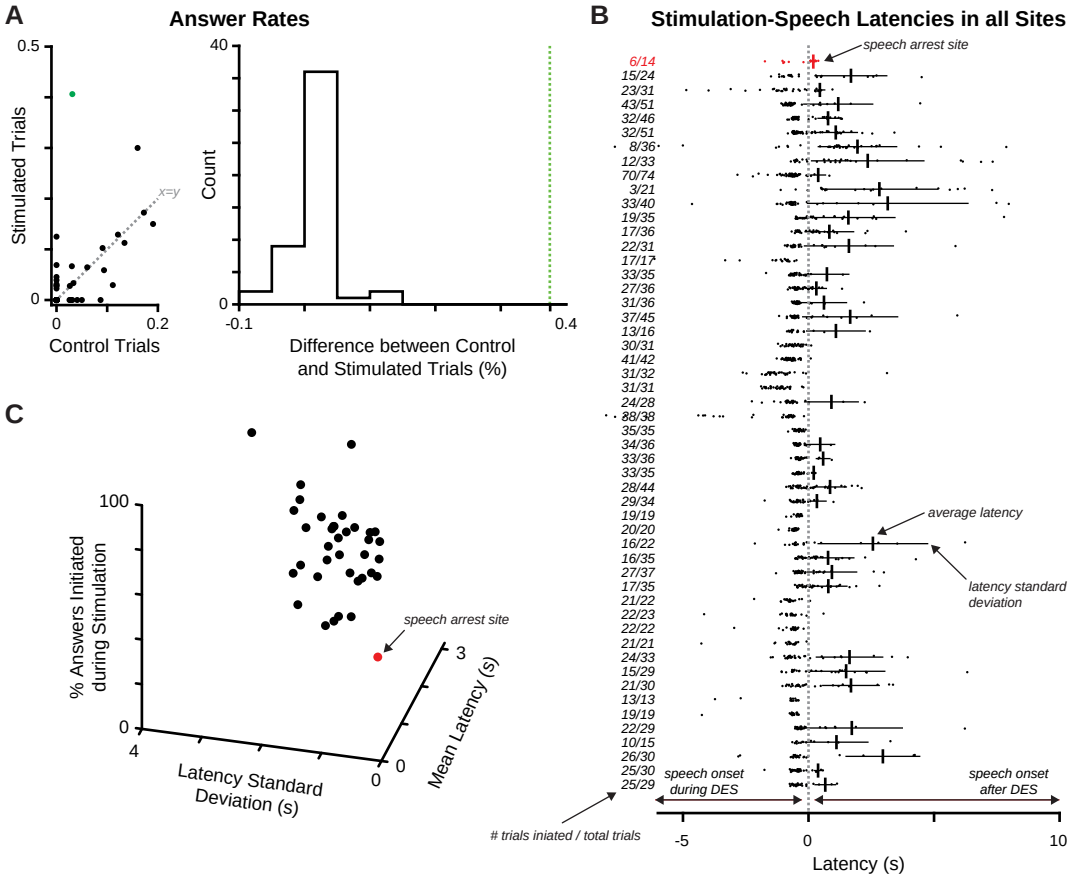

Figure S1. Additional quantification of stimulation-induced sensorimotor effects. (**A**) Proportion of control and stimulated trials answered (left) and the difference in answer rates (right) across participants; value related to site where stimulation induced perceptual deficits (see Fig. 1C,D) is indicated by green dashed line. (**B**) For all stimulation sites, mean stimulation-speech latency ± 1 standard deviation for trials where speech onset occurred after stimulation offset, with the proportion of trials answered while stimulation was ongoing at left; data for each site is presented in rows with dots representing latencies for individual trials. (**C**) Scatterplot reporting stimulation-speech latency summary statistics for each site.

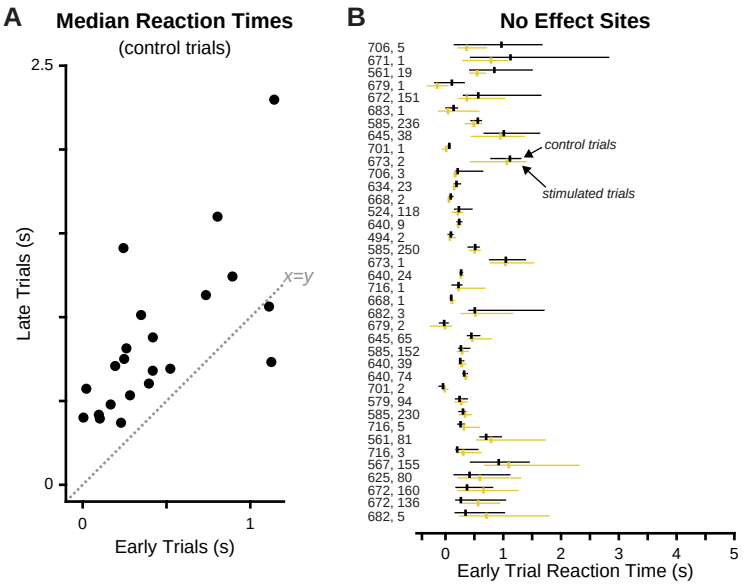

Figure S2. Additional quantification of reaction time. (**A**) For each participant, the median reaction time for all control trials pooled across stimulation sites when the CI was presented either question-medially (early) or question-finally (late); the median reaction time in early trials was significantly shorter than late trials across participants ($p = 0.0002$, sign-rank test). (**B**) Median reaction time and interquartile range for all sites where stimulation did not significantly affect reaction time; participant and site number indicated in leftmost column (i.e., participant #, site #).

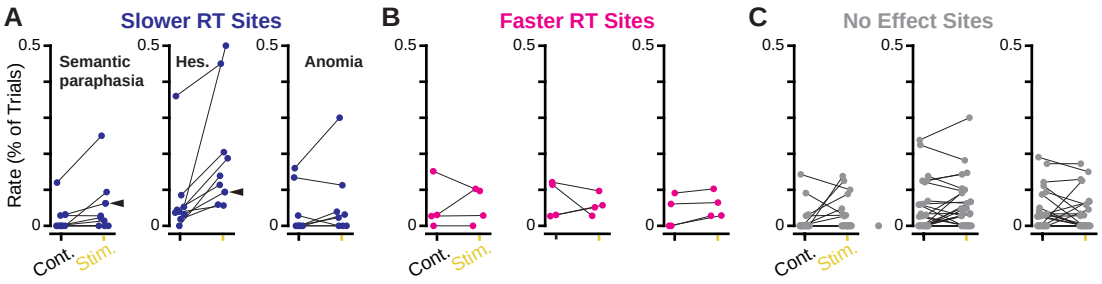

Figure S3. Error rates in sites according to stimulation-induced effects on reaction time. The rates of semantic paraphasia, hesitations, and anomia in control and stimulated trials for all sites where stimulation resulted in slower reaction times (RT) (**A**), faster RT (**B**), or no effect on RT (**C**). The site which also displayed stimulation-induced perceptual deficits (see Fig. 1C,D) was excluded from analyses of anomia and is indicated with an arrow on plots related to other error types.

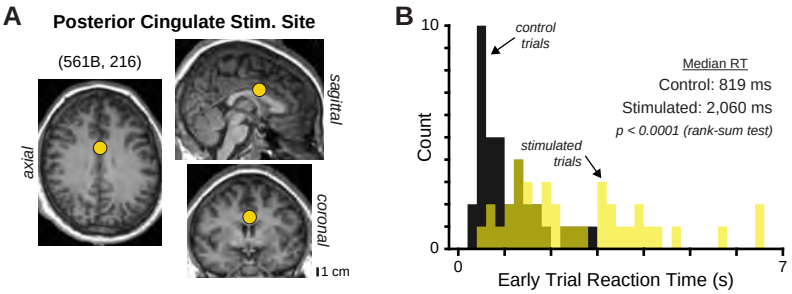

Figure S4. Slower reaction times resulting from posterior cingulate stimulation. (**A**) Preoperative magnetic resonance images depicting the stimulation site within posterior cingulate gyrus. (**B**) Histogram of RT in control trials and trials when the site in (A) was stimulated.

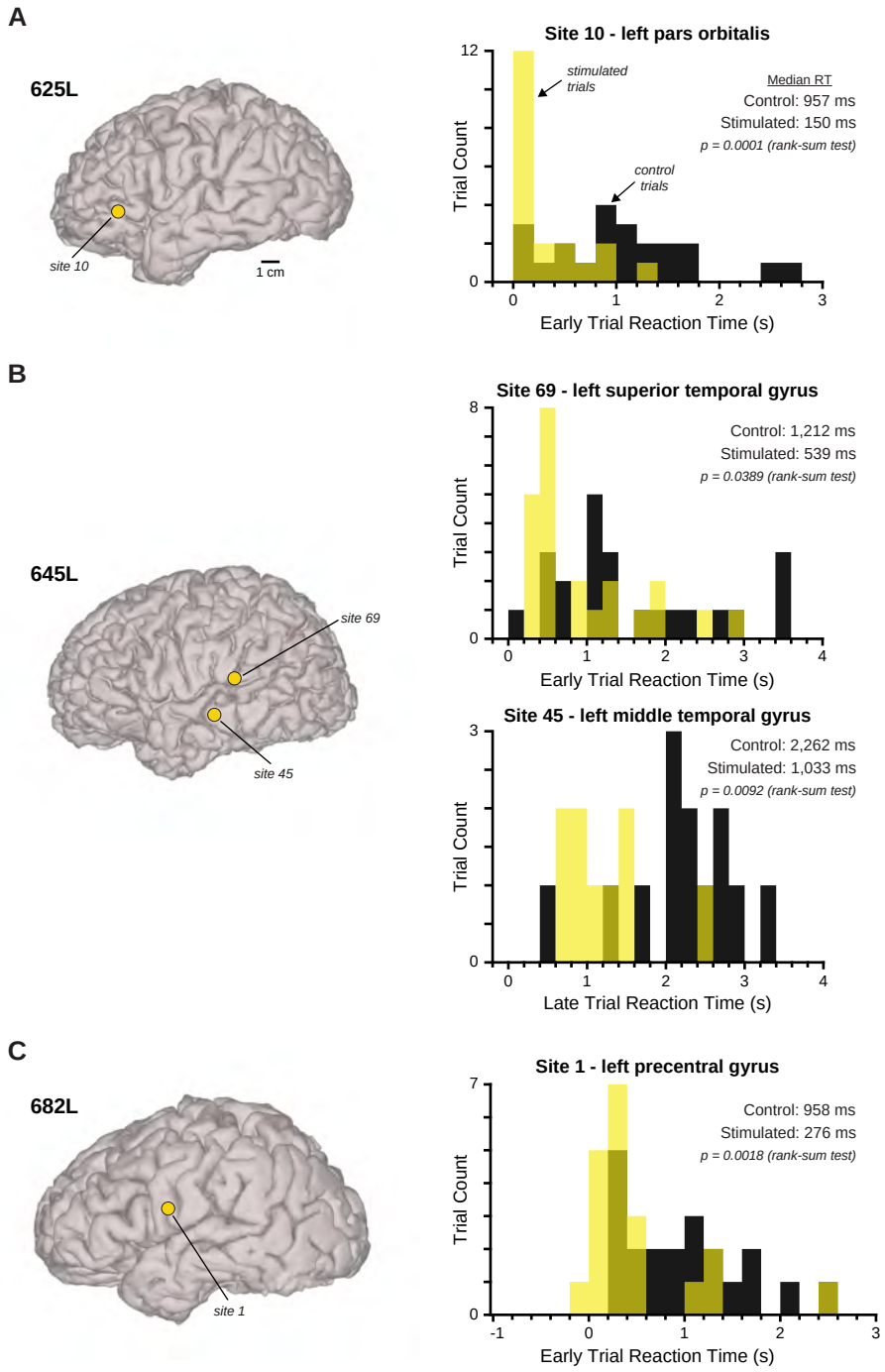

Figure S5. Sites exhibiting stimulation-induced faster reaction times. (**A-C**) Cortical surfaces from participants 625L (**A**), 645L (**B**), and 682L (**C**) depicting the location of sites where stimulation resulted in significantly faster reaction times (left), with histograms of reaction times in control and stimulated trials for each site (right).

Table S1 - Participant demographics and clinical information

Number	Age	Sex	Stimulator Type	Language Dominance (Method)	Handedness	Pathology/Diagnosis	Tumor Location/Seizure Loci	Notes
460L	51	M	Chronic subdural ECoG	LH (Wada testing)	right	Epilepsy (gliosis)	Left mesial temporal lobe	
494L	30	M	Acute Handheld	LH (Wada testing)	right (+70)	Hippocampal sclerosis (epilepsy)	Left hippocampus	
524R	18	M	Chronic SEEG	LH (fMRI)	left (-30)	Epilepsy	Bilateral multifocal	
561B	19	M	Chronic SEEG	LH (fMRI)	right	Epilepsy	Right parieto-occipital lobe	
567R	33	M	Chronic SEEG	Unknown	right (+90)	Epilepsy	Right peri-sylvian (posterior frontal-anterior parietal medial operculum/posterior insula)	
579B	12	F	Chronic SEEG	Unknown	left	Epilepsy	Right occipital	
585L	38	F	Chronic subdural ECoG	LH (Wada testing)	right	Epilepsy	left middle hippocampus	
625L	22	F	Chronic SEEG	Bihemispheric (Wada testing)	right	Epilepsy	left anterior medial temporal lobe	
634L	20	F	Chronic SEEG	LH (Wada testing)	right	Epilepsy	left amygdala and hippocampus and insula	
641L	37	M	Acute Handheld	Unknown	right (+70)	Astrocytoma	left frontal	Stimulation timing was estimated using from video of stimulator
645L	40	F	Chronic SEEG	Bihemispheric (Wada testing)	mixed	Epilepsy; Hydrocephalus	bilateral amygdala	
640L	43	F	Chronic SEEG	Bihemispheric (Wada testing)	right	Epilepsy	left amygdala	Patient reported occassional perception of scalp tingling during experiment, but did not appear to relate to stimulation delivery
668L	55	F	Acute Handheld	Unknown	right	Glioblastoma Multiforme	left parietal	
673R	43	M	Acute Handheld	Unknown	right	Glioblastoma Multiforme	right frontal (precentral gyrus)	
671DBS	71	M	Acute subdural ECoG	Unknown	right	Parkinson's Disease	N/A	
679L	57	F	Acute Handheld	Unknown	right	Esophageal CA metastasis; Hydrocephalus	Left frontoparietal	
683DBS	71	F	Acute subdural ECoG	Unknown	right	Parkinson's Disease	N/A	
684DBS	54	F	Acute subdural ECoG	Unknown	right	Parkinson's Disease	N/A	Vietnamese native speaker (English L2); CI task data not analyzed for stimulation effects in reaction time or errors and second stimulation site lacking gross motor deficits was not analyzed
682DBS	68	M	Acute subdural ECoG	Unknown	right	Parkinson's Disease	N/A	
672B	34	F	Chronic SEEG	LH (Wada testing)	right	Epilepsy	Right mesial temporal lobe	
701L	67	M	Acute Handheld	Unknown	right	Lung CA Metastasis	Left temporal lobe	
706DBS	56	F	Acute subdural ECoG	Unknown	right	Essential Tremor	N/A	
716DBS	51	M	Acute subdural ECoG	Unknown; speech motor site on left precentral gyrus	left	Essential Tremor	N/A	

Table S2 - Additional stimulation site information

Participant	Site	CIT168 Coregistered Coordinates			DKT Label	Condition	Reaction Time				Semantic Paraphasia		Anomia		Hesitations		Neologisms		Result Summary
		X	Y	Z			Early CI Trials (s)	p-value	Late CI Trials (s)	p-value	#	Rate	#	Rate	#	Rate	#	Rate	
460	204, Contact 1	-46.89	43.22	24.51	left pars triangularis	Control	**0.374**	**0.0088**	**0.675**	**0.0095**	**0**	**0**	**0**	**0**	**2**	**0.044**	0	0	**slower reaction times; increased errors**
	204, Contact 2	-52.93	37.73	16.39	left caudal middle frontal gyrus	Stimulated	**0.555**		**1.635**		**1**	**0.023**	**1**	**0.023**	**5**	**0.114**	0	0	
494	1, Contact 1	-57.26	25.85	3.86	left pars triangularis	Control	**0.133**	**0.0010**	**0.373**	**0.0003**	**1**	**0.031**	N/A	N/A	**1**	**0.031**	0	0	**slower reaction times; increased errors; perceptual deficits**
	1, Contact 2	-57.69	19.43	-1.98	left pars triangularis	Stimulated	**0.454**		**0.785**		**2**	**0.063**	N/A	N/A	**3**	**0.094**	0	0	
	2, Contact 1	-56.66	25.91	7.55	left pars triangularis	Control	0.094	0.8197	insufficient trials		**0**	**0**	**0**	**0**	0	0	0	0	increased errors
	2, Contact 2	-55.12	14.94	4.41	left pars opercularis	Stimulated	0.078				**2**	**0.125**	**2**	**0.125**	0	0	0	0	
	3, Contact 1	-60.71	11.91	10.79	left precentral gyrus	Control	N/A	N/A	N/A	N/A	N/A	N/A	N/A	N/A	N/A	N/A	N/A	N/A	**motor deficit (speech arrest)**
	3, Contact 2	-60.63	5.75	7.32	left precentral gyrus	Stimulated	N/A		N/A		N/A	N/A	N/A	N/A	N/A	N/A	N/A	N/A	
	4, Contact 1	-62.36	2.01	12.31	left precentral gyrus	Control	N/A	N/A	N/A	N/A	N/A	N/A	N/A	N/A	N/A	N/A	N/A	N/A	**motor deficit (dysarthria)**
	4, Contact 2	-66.41	-7.89	8.65	left precentral gyrus	Stimulated	N/A		N/A		N/A	N/A	N/A	N/A	N/A	N/A	N/A	N/A	
524	118, Contact 1	35.96	-22.06	17.88	right insula	Control	0.232	0.2675	insufficient trials		**0**	**0**	0	0	3	0.059	0	0	increased errors
	118, Contact 2	40.88	-20.78	20.23	right postcentral gyrus (parietal operculum)	Stimulated	0.214				**1**	**0.027**	0	0	0	0	0	0	
	82, Contact 1	37.44	8.03	57.37	right caudal middle frontal gyrus	Control	**0.195**	**5.17E-06**	**0.329**	**0.0058**	0	0	**0**	**0**	**1**	**0.019**	0	0	**slower reaction times; increased errors**
	82, Contact 2	42.43	9.88	59.37	right caudal middle frontal gyrus	Stimulated	**0.840**		**0.741**		0	0	**2**	**0.039**	**3**	**0.059**	0	0	
561	19, Contact 1	7.06	-22.97	29.95	right posterior cingulate gyrus	Control	0.846	0.1152	insufficient trials		0	0	0	0	2	0.059	0	0	no effect
	19, Contact 2	9.79	-22.44	33.49	right posterior cingulate gyrus (white matter)	Stimulated	0.547				0	0	0	0	1	0.028	0	0	
	216, Contact 1	-0.36	0.43	31.63	left posterior cingulate gyrus	Control	**0.818**	**6.16E-07**	insufficient trials		0	0	0	0	**4**	**0.085**	0	0	**slower reaction times; increased errors**
	216, Contact 2	-4.35	1.67	33.78	left posterior cingulate gyrus	Stimulated	**2.060**				0	0	0	0	**9**	**0.205**	0	0	
	225, Contact 1	-30.93	11.95	50.83	left caudal middle frontal gyrus	Control	**0.667**	**0.0156**	1.126	0.9654	0	0	0	0	**2**	**0.039**	0	0	**slower reaction times; increased errors**
	225, Contact 2	-35.77	10.24	52.16	left caudal middle frontal gyrus	Stimulated	**0.874**		1.073		0	0	0	0	**9**	**0.188**	0	0	
	81, Contact 1	57.77	33.36	5.07	right pars triangularis	Control	0.704	0.5169	insufficient trials		0	0	0	0	0	0	0	0	no effect
	81, Contact 2	63.78	32.52	10.09	right pars triangularis	Stimulated	0.790				0	0	0	0	0	0	0	0	
567	155, Contact 1	33.07	12.80	65.59	right caudal middle frontal gyrus	Control	0.922	0.1495	2.297	0.4807	0	0	2	0.041	11	0.224	0	0	no effect
	155, Contact 2	39.04	10.59	65.61	right caudal middle frontal gyrus	Stimulated	1.094		1.398		0	0	0	0	8	0.182	0	0	
	177, Contact 1	36.67	7.94	51.59	right caudal middle frontal gyrus	Control	N/A	N/A	N/A	N/A	N/A	N/A	N/A	N/A	N/A	N/A	N/A	N/A	**motor deficit (head and gaze movement)**
	177, Contact 2	41.72	7.48	54.76	right caudal middle frontal gyrus	Stimulated	N/A		N/A		N/A	N/A	N/A	N/A	N/A	N/A	N/A	N/A	
579	46, Contact 1	-49.91	-3.15	46.59	left precentral gyrus	Control	N/A	N/A	N/A	N/A	N/A	N/A	N/A	N/A	N/A	N/A	N/A	N/A	**motor deficit (head and gaze movement)**
	46, Contact 2	-52.17	-1.99	47.12	left precentral gyrus	Stimulated	N/A		N/A		N/A	N/A	N/A	N/A	N/A	N/A	N/A	N/A	
	94, Contact 1	-48.95	33.60	3.88	left pars triangularis	Control	0.243	0.8644	insufficient trials		0	0	0	0	**0**	**0**	0	0	increased errors
	94, Contact 2	-52.24	35.60	6.22	left pars triangularis	Stimulated	0.272				0	0	0	0	**1**	**0.067**	0	0	
585	152, Contact 1	-15.69	72.19	-8.47	left frontal pole	Control	0.267	0.5487	insufficient trials		0	0	0	0	**0**	**0**	0	0	increased errors
	152, Contact 2	-25.21	69.34	-7.39	left frontal pole	Stimulated	0.288				0	0	0	0	**1**	**0.032**	0	0	
	230, Contact 1	-41.14	19.83	56.73	left caudal middle frontal gyrus	Control	0.303	0.2032	insufficient trials		0	0	0	0	**0**	**0**	0	0	increased errors
	230, Contact 2	-49.12	9.18	56.10	left caudal middle frontal gyrus	Stimulated	0.337				0	0	0	0	**2**	**0.049**	0	0	
	236, Contact 1	-50.16	32.65	33.25	left caudal middle frontal gyrus	Control	0.560	0.2474	insufficient trials		0	0	0	0	2	0.069	0	0	no effect
	236, Contact 2	-56.41	27.46	26.59	left caudal middle frontal gyrus	Stimulated	0.489				0	0	0	0	2	0.063	0	0	
	250, Contact 1	-57.67	32.62	-4.80	left pars orbitalis	Control	0.514	0.6182	insufficient trials		0	0	0	0	0	0	0	0	no effect
	250, Contact 2	-59.95	27.06	5.76	left pars triangularis	Stimulated	0.503				0	0	0	0	0	0	0	0	
625	10, Contact 1	-48.70	34.63	-5.41	left pars orbitalis	Control	**0.957**	**0.0001**	1.169	0.4636	**1**	**0.030**	**3**	**0.091**	**1**	**0.030**	0	0	**faster reaction times; increased errors**
	10, Contact 2	-53.41	35.01	-4.12	left pars orbitalis	Stimulated	**0.150**		1.050		**4**	**0.103**	**4**	**0.103**	**2**	**0.051**	0	0	
	63, Contact 1	-52.01	7.50	33.84	left precentral gyrus	Control	N/A	N/A	N/A	N/A	N/A	N/A	N/A	N/A	N/A	N/A	N/A	N/A	**motor deficit (orofacial movement which the participant described as "a string pulling" face/mouth)**
	63, Contact 2	-57.65	7.33	35.08	left precentral gyrus	Stimulated	N/A		N/A		N/A	N/A	N/A	N/A	N/A	N/A	N/A	N/A	
	80, Contact 1	-38.00	19.54	6.79	left insula	Control	0.416	0.5089	1.243	0.9546	**0**	**0**	5	0.172	4	0.138	0	0	increased errors
	80, Contact 2	-39.56	23.26	11.24	left pars opercularis (frontal operculum)	Stimulated	0.593		1.045		**4**	**0.138**	5	0.172	3	0.103	0	0	
634	23, Contact 1	-3.75	32.34	19.90	left caudal anterior cingulate gyrus	Control	0.191	0.2424	0.459	1.0000	0	0	0	0	0	0	0	0	no effect
	23, Contact 2	-8.39	33.37	21.14	left caudal anterior cingulate gyrus	Stimulated	0.149		0.474		0	0	0	0	0	0	0	0	
	40, Contact 1	-40.76	2.38	41.06	left caudal middle frontal gyrus (precentral sulcus)	Control	**0.117**	**1.54E-07**	**0.439**	**0.0006**	1	0.029	1	0.029	**0**	**0**	0	0	**slower reaction times; increased errors**
	40, Contact 2	-46.15	2.85	41.36	left caudal middle frontal gyrus (precentral sulcus)	Stimulated	**3.445**		**2.663**		1	0.028	0	0	**5**	**0.139**	0	0	
640	24, Contact 1	55.02	-31.30	1.00	right superior temporal gyrus	Control	0.271	0.8467	0.524	0.0289	0	0	0	0	0	0	0	0	no effect
	24, Contact 2	60.42	-31.32	1.59	right superior temporal gyrus	Stimulated	0.263		0.433		0	0	0	0	0	0	0	0	
	39, Contact 1	-49.70	-0.59	-21.49	left superior temporal gyrus	Control	0.255	0.8090	0.525	0.4025	0	0	0	0	0	0	0	0	no effect
	39, Contact 2	-56.16	-0.64	-21.44	left middle temporal gyrus	Stimulated	0.280		0.486		0	0	0	0	1	0.028	0	0	
	74, Contact 1	-47.93	-28.91	9.84	left transverse temporal gyrus	Control	0.323	0.1424	0.535	0.7350	0	0	0	0	0	0	0	0	no effect
	74, Contact 2	-53.74	-28.25	11.52	left transverse temporal gyrus	Stimulated	0.349		0.490		0	0	0	0	0	0	0	0	
	90, Contact 1	-45.57	-29.35	-19.48	left fusiform gyrus	Control	**0.312**	**3.46E-07**	**0.563**	**0.0001**	**0**	**0**	**0**	**0**	**2**	**0.053**	0	0	**slower reaction times; increased errors**
	90, Contact 2	-50.95	-29.92	-20.13	left inferior temporal gyrus	Stimulated	**2.275**		**2.724**		**3**	**0.094**	**1**	**0.031**	**16**	**0.500**	0	0	
	9, Contact 1	54.13	0.73	-19.31	right middle temporal gyrus	Control	0.237	0.5301	0.510	0.9310	0	0	0	0	0	0	0	0	no effect
	9, Contact 2	60.00	0.44	-19.34	right middle temporal gyrus	Stimulated	0.221		0.418		0	0	0	0	0	0	0	0	
641	1, Contact 1	-56.48	31.29	20.92	left pars triangularis	Control	**0.346**	**0.0146**	1.013	0.3811	**0**	**0.000**	11	0.134	**3**	**0.037**	0	0	**slower reaction times; increased errors**
	1, Contact 2	-55.84	34.99	16.90	left pars triangularis	Stimulated	**0.578**		1.143		**1**	**0.014**	8	0.113	**4**	**0.056**	0	0	
645	38, Contact 1	-47.84	10.89	-28.31	left superior temporal gyrus	Control	1.009	0.2797	1.180	0.4303	0	0	0	0	**1**	**0.030**	0	0	increased errors
	38, Contact 2	-53.25	11.10	-29.38	left superior temporal gyrus	Stimulated	0.951		1.167		0	0	0	0	**4**	**0.091**	0	0	
	45, Contact 1	-51.18	-19.14	-11.73	left middle temporal gyrus	Control	0.730	0.4958	**2.263**	**0.0092**	1	0.027	**0**	**0**	**1**	**0.027**	0	0	**faster reaction times; increased errors**
	45, Contact 2	-58.39	-19.54	-11.27	left middle temporal gyrus	Stimulated	0.900		**1.033**		1	0.029	**1**	**0.029**	**2**	**0.057**	0	0	
	65, Contact 1	-41.52	-25.30	9.83	left transverse temporal gyrus	Control	0.448	0.3185	0.740	0.5114	0	0	1	0.026	1	0.026	0	0	no effect
	65, Contact 2	-47.53	-24.95	10.27	left transverse temporal gyrus	Stimulated	0.465		0.751		0	0	0	0	0	0.000	0	0	
	69, Contact 1	-68.04	-30.13	15.38	left superior temporal gyrus	Control	**1.212**	**0.0389**	1.704	0.1260	0	0	**0**	**0**	4	0.114	0	0	**faster reaction times; increased errors**
	69, Contact 2	-71.20	-31.88	15.50	left superior temporal gyrus	Stimulated	**0.539**		1.231		0	0	**1**	**0.028**	1	0.028	0	0	
668	1, Contact 1	-33.85	-60.14	63.71	left superior parietal cortex	Control	0.100	0.1564	insufficient trials		0	0	0	0	0	0	0	0	no effect
	1, Contact 2	-34.04	-63.45	61.21	left superior parietal cortex	Stimulated	0.110				0	0	0	0	0	0	0	0	
	2, Contact 1	-48.64	-44.08	61.29	left superior parietal cortex	Control	0.092	0.1433	insufficient trials		0	0	0	0	0	0	0	0	no effect
	2, Contact 2	-45.57	-44.74	65.00	left superior parietal cortex	Stimulated	0.060				0	0	0	0	0	0	0	0	
671	1, Contact 1	-60.51	20.10	7.58	left pars triangularis	Control	1.125	0.1285	insufficient trials		3	0.143	4	0.190	**5**	**0.238**	0	0	increased errors
	1, Contact 2	-59.33	22.19	15.29	left pars triangularis	Stimulated	0.788				2	0.100	3	0.150	**6**	**0.300**	0	0	
	3, Contact 1	-56.86	24.11	24.97	left caudal middle frontal gyrus	Control	**1.002**	**0.0191**	insufficient trials		**3**	**0.120**	**4**	**0.160**	**9**	**0.360**	0	0	**slower reaction times; increased errors**
	3, Contact 2	-53.65	26.31	32.11	left caudal middle frontal gyrus	Stimulated	**2.932**				**5**	**0.250**	**6**	**0.300**	**9**	**0.450**	0	0	
672	136, Contact 1	-49.18	3.16	-23.47	left superior temporal gyrus	Control	0.266	0.2798	0.981	0.9039	1	0.0278	4	0.111	0	0	0	0	no effect
	136, Contact 2	-54.09	3.26	-24.04	left middle temporal gyrus	Stimulated	0.565		0.993		1	0.0294	1	0.029	0	0	0	0	
	151, Contact 1	-64.12	-18.03	-9.49	left middle temporal gyrus	Control	0.568	0.3233	0.727	0.5181	0	0	1	0.027	1	0.027	0	0	no effect
	151, Contact 2	-68.60	-18.29	-8.29	left middle temporal gyrus	Stimulated	0.369		0.867		0	0	0	0	0	0	0	0	
	160, Contact 1	-59.34	-49.14	1.41	left middle temporal gyrus	Control	0.373	0.2798	0.702	0.2970	0	0	1	0.026	0	0	0	0	no effect
	160, Contact 2	-64.28	-50.10	2.47	left middle temporal gyrus	Stimulated	0.658		0.978		0	0	1	0.028	0	0	0	0	
673	1, Contact 1	45.64	-17.54	66.52	right precentral gyrus	Control	1.045	0.9440	insufficient trials		0	0	**0**	**0**	0	0	0	0	increased errors
	1, Contact 2	41.58	-15.82	67.58	right precentral gyrus	Stimulated	1.035				0	0	**1**	**0.045**	0	0	0	0	
	2, Contact 1	28.80	-10.88	74.55	right precentral gyrus	Control	1.115	0.5297	insufficient trials		0	0	0	0	0	0	0	0	no effect
	2, Contact 2	33.35	-11.87	73.08	right precentral gyrus	Stimulated	1.062				0	0	0	0	0	0	0	0	
679	1, Contact 1	-39.94	-21.80	67.02	left precentral gyrus	Control	0.110	0.2158	insufficient trials		**0**	**0**	1	0.050	**0**	**0**	0	0	increased errors
	1, Contact 2	-42.51	-20.31	63.58	left precentral gyrus	Stimulated	-0.145				**1**	**0.048**	0	0	**1**	**0.048**	0	0	
	2, Contact 1	-51.88	-11.48	51.06	left precentral gyrus	Control	-0.022	0.9342	insufficient trials		0	0	2	0.087	**0**	**0**	0	0	increased errors
	2, Contact 2	-53.99	-10.80	47.81	left precentral gyrus	Stimulated	-0.009				0	0	0	0	**2**	**0.100**	0	0	
682	1, Contact 1	-66.65	1.77	12.08	left precentral gyrus	Control	**0.958**	**0.0018**	insufficient trials		5	0.152	2	0.061	4	0.121	1	0.030	**faster reaction times**
	1, Contact 2	-65.44	6.50	19.54	left precentral gyrus	Stimulated	**0.276**				3	0.097	2	0.065	3	0.097	0	0	
	3, Contact 1	-62.29	10.66	28.29	left precentral gyrus	Control	0.508	0.7420	0.765	0.9015	**1**	**0.031**	3	0.094	**4**	**0.125**	0	0	increased errors
	3, Contact 2	-60.64	12.85	35.83	left precentral gyrus	Stimulated	0.520		0.881		**3**	**0.088**	2	0.059	**5**	**0.147**	0	0	
	5, Contact 1	-56.77	16.54	41.96	left caudal middle frontal gyrus	Control	0.347	0.2607	insufficient trials		0	0	**1**	**0.030**	2	0.061	0	0	increased errors
	5, Contact 2	-51.36	18.41	46.54	left caudal middle frontal gyrus	Stimulated	0.707				0	0	**2**	**0.067**	2	0.067	0	0	
683	1, Contact 1	-68.20	-24.11	38.50	left postcentral gyrus	Control	0.141	0.8245	insufficient trials		3	0.091	4	0.121	4	0.121	**0**	**0**	increased errors
	1, Contact 2	-63.91	-15.04	43.70	left postcentral gyrus (central sulcus)	Stimulated	0.042				1	0.032	4	0.129	3	0.097	**2**	**0.065**	
684	1, Contact 1	-68.04	-25.72	33.31	left inferior parietal cortex	Control	N/A	N/A	N/A	N/A	N/A	N/A	N/A	N/A	N/A	N/A	N/A	N/A	**motor deficit (involuntary vocalization)**
	1, Contact 2	-65.05	-17.86	39.50	left postcentral gyrus	Stimulated	N/A		N/A		N/A	N/A	N/A	N/A	N/A	N/A	N/A	N/A	
701	1, Contact 1	-67.47	-50.31	-2.13	left middle temporal gyrus	Control	0.066	0.0489	insufficient trials		0	0	0	0	0	0	0	0	no effect
	1, Contact 2	-68.49	-47.24	-2.97	left middle temporal gyrus	Stimulated	0.012				0	0	0	0	0	0	0	0	
	2, Contact 1	-66.80	-57.81	7.93	left middle temporal gyrus	Control	-0.043	0.0477	insufficient trials		0	0	0	0	0	0	0	0	no effect
	2, Contact 2	-67.72	-54.07	8.28	left middle temporal gyrus	Stimulated	-0.015				0	0	0	0	0	0	0	0	
706	1, Contact 1	-69.23	-10.86	-2.88	left superior temporal gyrus	Control	N/A	N/A	N/A	N/A	N/A	N/A	N/A	N/A	N/A	N/A	N/A	N/A	**motor deficit (dysarthria)**
	1, Contact 2	-65.64	-2.41	5.50	left precentral gyrus (lateral sulcus)	Stimulated	N/A		N/A		N/A	N/A	N/A	N/A	N/A	N/A	N/A	N/A	
	3, Contact 1	-64.64	5.74	14.36	left precentral gyrus	Control	0.212	0.0591	0.865	0.9682	0	0	0	0	1	0.033	0	0	no effect
	3, Contact 2	-62.80	11.22	21.40	left precentral gyrus	Stimulated	0.168		0.981		0	0	0	0	1	0.034	0	0	
	5, Contact 1	-56.87	16.60	31.52	left pars opercularis	Control	0.968	0.3865	insufficient trials		0	0	0	0	**2**	**0.125**	0	0	increased errors
	5, Contact 2	-53.30	24.38	41.35	left caudal middle frontal gyrus	Stimulated	0.365				0	0	0	0	**2**	**0.143**	0	0	
716	1, Contact 1	-58.10	35.85	0.56	left pars triangularis	Control	0.226	0.3348	0.651	0.3638	0	0	**0**	**0.000**	**0**	**0**	0	0	increased errors
	1, Contact 2	-57.40	35.93	13.43	left pars triangularis	Stimulated	0.226		0.501		0	0	**2**	**0.069**	**1**	**0.0345**	0	0	
	3, Contact 1	-54.37	37.11	23.28	left caudal middle frontal gyrus	Control	0.203	0.4034	0.661	0.7337	0	0	1	0.033	0	0	0	0	no effect
	3, Contact 2	-49.89	37.77	30.17	left caudal middle frontal gyrus	Stimulated	0.309		0.647		0	0	1	0.033	0	0	0	0	
	5, Contact 1	-46.60	38.48	37.23	left caudal middle frontal gyrus	Control	0.260	0.2892	0.809	0.2241	0	0	1	0.031	0	0	0	0	no effect
	5, Contact 2	-39.15	37.22	46.35	left caudal middle frontal gyrus	Stimulated	0.318		1.021		0	0	0	0	0	0	0	0	